Journal of Materials Science & Technology 135 (2023) 170–185

Contents lists available at ScienceDirect

Journal of Materials Science & Technology

journal homepage: www.elsevier.com/locate/jmst

Research Article

# The physiological polyphosphate as a healing biomaterial for chronic wounds: Crucial roles of its antibacterial and unique metabolic energy supplying properties

Werner E.G. Müller[a,1,*], Hadrian Schepler[b,1], Meik Neufurth[a], Shunfeng Wang[a], Veronica Ferrucci[c], Massimo Zollo[c,d], Rongwei Tan[e], Heinz C. Schröder[a], Xiaohong Wang[a,*]

[a] ERC Advanced Investigator Grant Research Group at the Institute for Physiological Chemistry, University Medical Center of the Johannes Gutenberg University, Duesbergweg 6, Mainz D-55128, Germany
[b] Department of Dermatology, University Clinic Mainz, Langenbeckstr. 1, Mainz D-55131, Germany
[c] Dipartimento di Medicina Molecolare e Biotecnologie Mediche, Università degli Studi di Napoli Federico II, Via Sergio Pansini 5, Naples 80131, Italy
[d] Ceinge Biotecnologie Avanzate Francesco Salvatore, Via G. Salvatore 486, Naples 80145, Italy
[e] Shenzhen Lando Biomaterials Co., Ltd., Shenzhen 518107, China

ARTICLE INFO

*Article history:*
Received 5 May 2022
Revised 21 June 2022
Accepted 12 July 2022
Available online 13 August 2022

*Keywords:*
Inorganic polyphosphate
Nanoparticles
Hydrogel
Coacervate
Human chronic wounds
Antibacterial activity
Metabolic energy

ABSTRACT

Insufficient metabolic energy, in the form of adenosine triphosphate (ATP), and bacterial infections are among the main causes for the development of chronic wounds. Previously we showed that the physiological inorganic polymer polyphosphate (polyP) massively accelerates wound healing both in animals (diabetic mice) and, when incorporated into mats, in patients with chronic wounds. Here, we focused on a hydrogel-based gel formulation, supplemented with both soluble sodium polyP (Na-polyP) and amorphous calcium polyP nanoparticles (Ca-polyP-NP). Exposure of human epidermal keratinocytes to the gel caused a significant increase in extracellular ATP level, an effect that was even enhanced when Na-polyP was combined with Ca-polyP-NP. Furthermore, it is shown that the added polyP in the gel is converted into a coacervate, leading to encapsulation and killing of bacteria. The data on human chronic wounds showed that the administration of hydrogel leads to the complete closure of these wounds. Histological analysis of biopsies showed an increased granulation of the wounds and an enhanced microvessel formation. The results indicate that the polyP hydrogel, due to its properties to entrap bacteria and generate metabolic energy, is a very promising formulation for a new therapy for chronic wounds.



## 1. Introduction

Wound healing of the skin reflects in an exemplary manner the power of the regenerative potential of living multicellular organisms. The ability to heal wounds is imperative for the evolution of the kingdoms Plantae (plants) and Metazoa (animals) [1]. Among the different organs in animals, the skin contributes ~15% of the body weight. The functions of the skin are manifold, as it acts as a barrier to protect the body against an exogenous physical, chemical, and bacterial environment foreign to the body. The surrounding media, primarily air and water, are loaded with a variety of noxious and destructive agents that can disrupt the structure and function of biological systems and interfere with the homeostatic circuits. It is fascinating that the toolkit of the skin cells and their surrounding extracellular matrix (ECM) is provided with the purging armory to resist damaging extra-individual attacks.

After injury of the physical, chemical, and/or bacterial skin barrier, wound healing processes proceed in a programmed manner. Traditionally, wound regeneration is divided into four overlapping phases hemostasis, inflammatory, proliferative, and reconstitution [2]. In the coagulation and hemostasis phase, an influx of leukocytes/immune cells occurs, leading to inflammation with signs of edema and erythema, during which lysosomal enzymes in concert with reactive oxygen species clean up cell debris before entering the proliferation and remodeling phase. The thrombocytes

* Corresponding authors.
*E-mail addresses:* wmueller@uni-mainz.de (W.E.G. Müller), wang013@uni-mainz.de (X. Wang).
[1] These authors contributed equally to this work.

https://doi.org/10.1016/j.jmst.2022.07.018

(blood platelets) are an integral component not only in the initial phases of wound healing but also during the complete progression of the process. They prevent blood loss at the site of injury, provide the platform for thrombin generation and fibrin formation and release biologically active proteins that promote and accelerate healing. Although they are anucleate, the platelets synthesize tissue factors such as interleukin-1$\beta$. They form a fibrin mesh in the ECM that chemotactically attracts stem cells that—after proliferation and migration—form the restored dermis/epidermis. Importantly, during all four phases of wound healing, platelets take part functionally and biochemically [3].

Only more recently, it has been shown that an inorganic polymer, polyphosphate (polyP), is a dominant component formed in the platelets and released during their activation [4]. Originally, polyP was identified as metaphosphoric acid in extracts of the nuclein from yeasts in 1890 [5]. This material has an amorphous phase and is associated with only very few impurities. Soon later Meyer [6] discovered the volutin granules in plants and bacteria, which are composed of metachromatic, highly refractive, and strongly basophilic bodies formed of polymetaphosphate [6]. PolyP was re-discovered by Langen et al. [7], Kornberg et al. [8], and Kulaev and Belozerskij [9,10]. Our group started to elucidate selected aspects of the biological and biomedical processes that are elicited by polyP in the early 90 s [11–13]. The polymer is synthesized in megakaryocytes from where the platelets develop. Intracellularly, polyP is present in nanoparticles (NPs) in the acidocalcisomes, most likely with $Ca^{2+}$ as a counterion [14]. Our group succeeded to fabricate similarly sized (100 nm) NPs, which are—like those within the cells—amorphous [15] and do not transform into the crystalline state [16]. They are formed from Na-polyP and $CaCl_2$ and were termed "Ca-polyP-NP". The polymer exists in animals *in vivo* predominantly with a chain length between 20 and 100 phosphate ($P_i$) units [10]. Long-chain polyP is found in bacteria with a chain length of 1000 $P_i$ residues and is associated with their virulence as in *Salmonella* spp., *Shigella flexneri*, or *Vibrio cholera* [17].

In spite of some controversial findings, which could be attributed to methodological problems, no adverse effects can be ascribed to polyP at the concentrations present in the blood [18]. Upon activation of the platelets, shorter chain length polyP molecules are released from the dense granules into the extracellular space, while longer polymers entrapped in NP remain associated on the platelet surface [19]. Extracellular polyP-NP are taken up by endocytosis, e.g., by human osteosarcoma SaOS-2 cells, as demonstrated in inhibitor experiments with trifluoperazine dihydrochloride [20,21].

The physiological polymer polyP has regenerative activity and accelerates the repair of hard and soft tissues as in bone [22,23] and cartilage [24]. In attempts to elucidate these morphogenetic processes, it was found that polyP stimulates tube formation of endothelial cells *in vitro*, an indication for induction of microvascularization [25]. This view was further substantiated by results indicating that during hydrolysis of polyP, human umbilical vein endothelial cells (HUVEC) interact chemotactically with each other under the formation of circular patterns of these cells with diameters of ~100 µm [21]. Further progress in elucidating the repair potential of polyP came from *in vivo* findings in both normal and diabetic mice, which revealed surprisingly rapid and complete healing of normal wounds and an almost complete restoration of skin injury in diabetic animals [26]. In continuation, individual unproven interventions in clinical practice started, which confirmed the very promising animal results [27]. The studies were performed with collagen mats into which calcium polyphosphate nanoparticles ("Ca-polyP-NP") were integrated (8 mg of NP/1 mL collagen solution). These mats stimulated the growth of keratinocytes and their differentiation to a microvillar phenotype. In addition, these cells showed a pronounced propensity to adhere and migrate and even to penetrate into the mats. Impressive acceleration of the re-epithelialization process has been observed in patients with chronic wounds. Complete healing was achieved after about 10 weeks. The regular replacement of the mats was flanked by the application of a moisturizing solution, also supplemented with polyP.

In the present report, the biochemical basis for the pronounced wound healing potential of the polyP-supplemented mats is mechanistically addressed. The rationale is based on previous findings that underscored the capacity of polyP to generate metabolic energy during the enzymatic degradation of the polymer. In earlier studies we demonstrated that polyP is hydrolyzed to single $P_i$ units with the enzyme alkaline phosphatase (ALP); the potential of ALP to degrade the polymer was reported in 2001 [28]. The individual $P_i$ units within the polyP chain are linked *via* high-energy phosphoanhydride linkages. In line with the discovery of Lippman [29], it has been established that during the cleavage of such a bond, a portion of the energy is lost as heat. However, in living organisms, at least a fraction of the liberated Gibbs free energy ($\Delta G$) is re-used for anabolic reactions, and by this, stored in biological systems as metabolically useful and convertible energy. This biochemical paradigm was supported by previous experiments, which showed that the exposure of osteoblast-like SaOS-2 cells to polyP-NP significantly upregulates both the intra- and extracellular ATP pool [30]. Furthermore, it was demonstrated that these cells comprise the ALP on the cell surface. In addition to ALP, the adenylate kinase (ADK), a phosphotransferase that catalyzes the interconversion of the adenosine phosphates ATP, adenosine diphosphate (ADP), and adenosine monophosphate (AMP), is localized on the external cell surface [31]. Consequently, inhibitor studies were performed to clarify the route of conversion of the released metabolic energy after ALP-mediated polyP hydrolysis. Applying levamisole (LEV) as an inhibitor of ALP and $P^1$,$P^5$-di(adenosine-5′)pentaphosphate ($Ap_5A$) as a potent blocker of ADK, it was verified that ADP is initially formed during ALP-mediated polyP degradation, which is subsequently up-phosphorylated to ATP [31]. This pathway was further confirmed by incubating the cells with apyrase, an enzyme that depletes the extracellular ATP pool [32], after which the directed migration of HUVEC is suppressed [21]. In wound healing, the cross-talk between keratinocytes and fibroblasts is pivotal for the successful and fast completion of this process. Interestingly enough, these cells are equipped with the enzymatic arsenal for interconverting AMP, ADP, and ATP and also expose P2 receptors, which act as receivers for these nucleotides and regulate downstream proliferation, differentiation, and apoptosis [33].

It is obvious that every cell involved in regenerative processes in the body needs metabolic energy, e.g., in form of glucose or ATP [34]. However, precise calorimetric measurements are missing. It has been outlined that calcium ions and carbonate ions are controlled with their respective pumps and channels and decisively contribute to functional repair processes [35]. Only recently, experimental evidence has been presented proving that both extracellular ATP and ADP promote wound healing. Free ATP and also its physiological storage form, polyP, were proven to improve wound healing. ATP, when encapsulated in gold NP, promotes wound healing in both normal and diabetic mice (reviewed in Ref. [36]). The physiological polymer polyP, which was identified as an extracellular ATP generator [37], accelerates wound healing in normal/diabetic mice [26] and also in humans and in patients [27]. ADP has a functional role in hemostasis and platelet aggregation and activates purine and purinergic receptors, $P2Y_1$, $P2Y_{12}$, and $P2Y_{13}$, on immune cells and keratinocytes, thereby promoting wound healing in diabetic mice (see Ref. [38]).

It is important to mention that in chronic and diabetic wounds, ATP deficiency is a key factor contributing to delayed or absent wound regeneration [39]. In the tissue of such patients, the re-

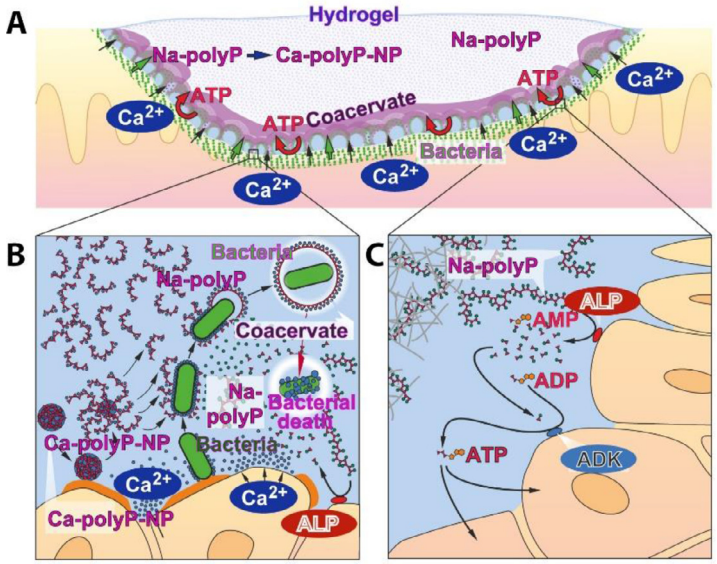


**Fig. 1.** Schematic outline of the transformations/phase transitions of polyP in the hydroxyethyl cellulose-based hydrogel. (A) Formation of "Ca-polyP-NP" from Na-polyP in the hydrogel. The killing of the bacteria, the coacervate formation, and the ATP generation at the border between the injured tissue and the wound gel are sketched. (B) Coacervate formation from Na-polyP in the gel and $Ca^{2+}$ extruded from the wound exudate causing the death of bacteria. (C) Formation of ATP *via* AMP and ADP from polyP driven by the enzymes ALP and ADK.

duction in the ATP pool is about 80%. Another biochemically neglected parameter in delayed wound healing is bacteria that interfere with wound regeneration. The dominant bacteria colonizing infected wounds are *Staphylococcus aureus* (37%), *Pseudomonas aeruginosa* (17%), *Proteus mirabilis* (10%), and *Escherichia coli* (6%) [40]. All of them, *S. aureus* [41], *P. aeruginosa* [42], *P. mirabilis* [43], and *E. coli* [44], are pore-forming microbes. The well-studied species *S. aureus* with its major virulence factor, the pore-forming alpha-toxin (hemolysin A), which is secreted [45], inserts 1.4 nm small pores into cells of the wounded cell layers, leading to a decrease in the intracellular ATP pool [46]. Frequently cell death is the consequence of those bacterial impact(s) [47]. ATP deprivation in the intracellular and also extracellular space is a major signaling and metabolic cause of cell death [48]. Therefore, it is rational to imagine that substitution of the environment of cells in the wound bed with either ATP or another metabolic high-energy (e.g., phosphate) compound should be beneficial and represent a major key to accelerating wound regeneration.

A further beneficial property of polyP is its transformation from a fluid/suspensory phase into a coacervate [49]. During this phase transition, polyP changes into an aqueous gel-like paste through liquid-liquid phase separation. Importantly, this coacervate state is the physiological, functionally, and morphogenetically active forms of the polymer, allowing mesenchymal stem cells to invade the polymer [49,50]. In a previous investigation, a collagen mat supplemented with polyP was applied to chronic wounds to demonstrate the effectiveness of this physiological polymer [27]. In the present work, polyP was integrated into a gel matrix to extend its potential and exploit the antibacterial property of polyP. Due to its pronounced biodegradability and biocompatibility together with its non-toxicity, the linear polysaccharide cellulose, composed of 1,4-$\beta$-D-glucopyranosyl units, was selected. Hydroxyethyl cellulose (HEC) was applied in order to stabilize the strong intra- and inter-chain hydrogen bonds. In addition, HEC is approved as a stabilizer, thickener, and coating material for pharmaceutical and cosmetic use and especially as wound dressing [51]. By this, the gel protects the wound as a physical barrier against the external environment, supplements the wound dressing with ATP, keeps the wound moist and absorbs cell debris, as well as supports autolysis of cells including bacteria in the exudate, through embedding into the coacervate (Fig. 1).

Embedded in the hydrogel are Na-polyP and "Ca-polyP-NP", which serve as a depot for the release of soluble polyP. As documented under "Results", the embedment of the physiological polymer polyP in the gel formulation leads to coacervation of polyP in the wound area (Fig. 1(A)). This phase transition of polyP results in the transformation of polyP into the physiologically active coacervate form that elicits morphogenetic activity supporting the regeneration process for wound healing [27]. In addition, in the coacervate envelope the bacteria are killed, most likely due to deprivation of $Ca^{2+}$ [52] (Fig. 1(B)). In parallel, ATP is formed from polyP as a result of the action of the enzymes ALP and ADK (Fig. 1(C)).

Taken together, the data presented underscore the unusual potential of polyP as a very useful, multi-acting ingredient in the successful management of chronic and difficult-to-heal open wounds.

## 2. Experimental section/methods

### 2.1. Materials

Na-polyphosphate (Na-polyP) with an average chain length of 40 $P_i$ units was purchased from Chemische Fabrik Budenheim (Budenheim; Germany).

### 2.2. Fabrication of Ca-polyP-NP

Amorphous nanoparticles of Ca-polyP were prepared as described [15]. A solution of 1 g of Na-polyP/25 mL of distilled water was dropped into a solution of 3.86 g of $CaCl_2 \cdot 6H_2O$ (#A537.1; Roth, Karls-ruhe; Germany) per 25 mL of water. The pH was kept at 10. After stirring for 12 h, the particles were filtered off and washed sequentially in water and ethanol and then dried (50 °C). The sample was termed "Ca-polyP-NP".

### 2.3. Formulation of the polyP-containing hydrogel

A suspension of polyP (200 mg of Na-polyP and 20 mg of "Ca-polyP-NP" per 10 ml) was prepared in purified water, followed by

15 min ultrasonication in a water bath. The suspension was filtered through a 0.2 µm PES membrane (#83.1826.001; Sarstedt; Nümbrecht; Germany). In parallel, 2 g of hydroxyethyl cellulose (HEC; Caelo, Hilden; Germany; #4482 - NATROSOL250 HX Pharm) were suspended in 20 g of 1,2-propandiol (#2554; Caelo). Afterwards, 65 g of purified water, as well as 10 g of phosphate buffer pH 6.5, were added slowly with stirring. This sample was heated to 121 °C under overpressure (1 bar). In the end, 3 mL of the polyP suspension were added to give a final concentration of 600 $\mu$g/mL of Na-polyP and 60 $\mu$g/mL of "Ca-polyP-NP". This formulation was blended in a roll mixer for 45 min. The final pH of the formulation was 6.5. This 2% (w/v) hydrogel containing polyP was termed "polyP-hydrogel" and the polyP-lacking hydrogel was termed "hydrogel".

The gels were prepared under sterile conditions starting from autoclaved (121 °C; 1 bar positive pressure; 20 min) components. The pH was ~6.5. At the end and after cooling down to 23 °C, the polyP components were added. Aliquots of the gels were stored in 10 mL syringes (# 4617100 V; B. Braun, Melsungen; Germany) with a Luer Lock adapter and sealing cap.

### 2.4. Fabrication of collagen-based mats

The preparation procedure for wound coverage has been recently described [27]. Bovine collagen (type I) provided by Lando Biomaterials (Shenzhen; China) was processed *via* a sequential acid/neutral pH treatment to allow the organization of the collagen fibrils. Then 8 mg of "Ca-polyP-NP" were added to 1 mL collagen solution and the resulting mats were washed with phosphate buffered saline (PBS). After a rapid transfer to ethanol (70%; v/v), the mats were sandwiched between two filter paper stacks (Whatman-3MM-blotting paper). The respective piles were overlayed with a nylon mesh filter (100 $\mu$m) and loaded with 20 g for 20 min; during this process, the mats were compressed to a thickness of 1 to 1.3 mm and stored in 70% (*v*/*v*) ethanol; "Ma/Col-Ca-polyP-NP".

### 2.5. Viscosity studies

The studies were performed with a Brookfield/PCE-RVI 1 viscometer (PCE Instruments, Meschede; Germany) as described [53–55]. Two temperatures were selected; 23 °C (room temperature) and 37 °C (human body temperature). The dynamic viscosity is given in Pa s in the solution mentioned, supplemented with 2% (w/v) HEC. The average viscosity of HEC, specified by the company as NATROSOL250 (Caelo), is listed with 10.8 Pa s. The system follows a non-Newtonian fluid situation since the viscous stresses that occur do not linearly correlate with the local strain rate [56].

### 2.6. Microscopic analyses

As described earlier [27], the environmental scanning electron microscope (ESEM) observations were performed with a Philips microscope (Eindhoven; Netherlands) and the scanning electron microscope (SEM) studies with a Zeiss Gemini 1530 (Zeiss, Oberkochem; Germany). The samples were freeze-dried prior to inspection. The light microscopical images were taken with a VHX-600 Digital Microscope (Keyence, Neu-Isenburg; Germany).

### 2.7. Staphylococcus aureus cultivation

The conditions have been described earlier [57,58]. The stock sample of *Staphylococcus aureus*, NCTC 13143, was obtained from DZIF (Braunschweig; Germany). The bacteria were cultivated in liquid cultures with tryptic soy broth (TSB) medium (Merck, Darmstadt; Germany) or in BD brain heart infusion agar with 10% sheep blood (Becton Dickinson, Heidelberg; Germany). The final $Ca^{2+}$ composition of the brain heart infusion agar/sheep blood was 0.4 mM. Where indicated and to compensate for a potential depletion of $Ca^{2+}$ by the chelator polyP, the $Ca^{2+}$ level in the medium was supplemented with an additional 5 mM $CaCl_2$. For the cultivation onto the hydrogel, the bacteria were grown first in liquid culture overnight until an $OD_{600\ nm}$ of 0.6 was reached. Then aliquots of 100 µL (for 5 cm dishes; Greiner-Sigma) or 300 µL (for 10 cm dishes; Greiner-Sigma) were spread out. As indicated, the dishes were layered with 150 µL of a hydrogel sample per 5 cm dish. Then the cultures were incubated for 120 min.

### 2.8. S. aureus *inhibition*

Qualitative testing for antibacterial activity was performed using the paper disk assay as described before [59–61]. The bacteria were cultivated on infusion agar containing 10% sheep blood. For this, the agar was plated into 10 cm dishes and overlayed with a *S. aureus* overnight culture suspension (100 µL). The plates were allowed to air dry for 10 min and then covered with 200 µL of a 10 mM $CaCl_2$ solution. After a further drying cycle, sterile paper discs (Whatman 3 MM; Fisher Scientific, Schwerte; Germany) with a diameter of 5 mm were attached to the surface of the culture. Finally, increasing concentrations of Na-polyP and, if indicated, also "Ca-polyP-NP" dissolved/suspended in saline were pipetted onto the discs (20 µL). Incubation was performed at 37 °C for 15 h and the plates were inspected by light microscopy. The diameter of the inhibition zone was measured and the plates were photographed.

The quantitative determination of the antibacterial activity caused by polyP in the hydrogels was performed as follows [62,63]. An overnight culture of *S. aureus* was cultivated in a TSB medium and the bacteria were harvested at the mid-exponential growth phase by centrifugation (2000 g, 10 min). After adjusting the resuspended *S. aureus* suspension to a density of $10^8$ colony-forming units (CFU)/mL in brain infusion agar with 10% sheep blood, the bacteria sample was used for the assay. This medium was supplemented with 5 mM $CaCl_2$. The fabricated hydrogel samples were diluted with 15 mM phosphate buffer down to a concentration of 30% (w/v) and 200 µL aliquots were added to 48-well plates. Subsequently, 200 µL of the bacterial suspension was added to the hydrogel samples. After incubation at 37 °C for 24 h, the reduction of bacteria density was determined by the colony-counting method [64]. The CFU counts obtained with the "polyP-hydrogel" samples were compared with those measured in the corresponding "hydrogel" assays.

### 2.9. Cultivation of cells (keratinocytes and A549 cells)

Human non-transformed adult skin epidermal keratinocytes [65] and adenocarcinomic human alveolar basal epithelial cells A549 [66] were used.

The keratinocytes were obtained from Sigma-Aldrich (#102–05A) and cultivated in a complete epidermal keratinocyte culture medium (#SCMK001, Sigma-Aldrich) as outlined before [67,68]. The A549 cells were kept in Dulbecco's modified Eagle's medium (DMEM; Sigma) with 10% fetal calf serum (FCS; Biochrom GmbH, Berlin; Germany) as described [69]. The culture medium/serum was supplemented with 5 mM $CaCl_2$ in order to prevent chelation through the polyP polymer. The cells were seeded at a density of 10,000 cells/$cm^2$ (1 mL) in 8-well plates grown in a humidified atmosphere of 5% $CO_2$ in air (37 °C). Every 3 to 4 d the medium/serum was replaced.

The response of polyP on the attachment pattern was determined in 48-well plates coated with 100 µL hydrogel. Then, a 300 µL suspension of keratinocytes ($10 \times 10^3$ cells/mL) was layered

on top of the hydrogel. After 24 h, the cell layer was inspected by Nomarski phase contrast optics (Olympus IX70 microscope).

Under the same conditions, also A549 cells were layered onto the hydrogel layer. Then 300 µL of a cell suspension ($7.5 \times 10^3$ cells/mL) was added and after a 24-h incubation period the cell layer was stained with Calcein-AM (#C1359, Sigma-Aldrich) [70].

### 2.10. ATP determination in the extracellular space

Adult skin epidermal keratinocytes were used in this study. Cells at a density of $5 \times 10^5$ cells/mL were seeded into 48-well plates coated with 100 µL gel, either "hydrogel" or polyP-containing "polyP-hydrogel" supplemented with different concentrations of Na-polyP or/and "Ca-polyP-NP". After a pre-incubation period of 2 h onto the respective hydrogel at 37 °C in the incubator, the assays were supplemented with 300 µL of epidermal keratinocyte culture medium, and incubation was continued for an additional 2 h.

Where indicated, inhibitors were added in a volume of 300 µL (in culture medium) in the following final concentrations; 20 $\mu$M trifluo-perazine dihydrochloride (TFP; #T8516 Sigma) or a mixture of 1 mM (−)-tetramisole hydrochloride (LEV; #L9756 Sigma) together with 40 $\mu$M $P^1$,$P^5$-di(adenosine-5′)pentaphosphate ($Ap_5A$; pentasodium salt; #D4022, Sigma) prior to the addition of the cells. TFP is a blocker of clathrin-dependent endocytosis [71], LEV is an inhibitor of ALP [72], and $Ap_5A$ suppresses the ADK reaction [73]. After incubation, the samples were spun down (500 g, 3 min). The supernatant was collected, aliquoted ($2 \times 100$ µL), and frozen at –80 °C. In order to inactivate the enzymes, 0.5 mM Pefablock (Biomol GmbH, Hamburg; Germany) was added.

ATP was quantitated using the ATP-monitoring luminescence assay (No. LL-100-1; Kinshiro, Toyo; Japan) as described [31,33,74]. The ATP concentration is given in pmol/$10^6$ cells. The number of viable cells was determined with the Trypan Blue (#T8154 Sigma-Aldrich) exclusion test [75].

### 2.11. Cell viability assay

The fast cell viability indicator PrestoBlue was used, which reduces resazurin to fluorescent resorufin in living cells [76]. A549 cells were seeded into 48-well plates coated with a hydrogel layer (2% HEC) (100 µL per well). The hydrogel was supplemented with different concentrations of either Na-polyP or "Ca-polyP-NP", which were added separately or as a mixture to the hydrogel. The concentrations are given with the respective assays. Then, a 300 µL suspension of A549 cells ($7.5 \times 10^3$ cells/mL) was added. The incubation was limited to 72 h. Then, the cultures were reacted with the colorimetric assay solution PrestoBlue (#A13261; Invitrogen/Thermo Fisher Scientific, Dreieich; Germany) as described [77]. Finally, the change of color was measured at an excitation wavelength of 544 nm and an emission wavelength of 590 nm. The results are given in absolute fluorescence units (AFU). Ten parallel experiments were performed. Data given are means ± SD ($^*p < 0.01$).

### 2.12. Application of polyP-containing hydrogel for chronic wounds

In order to re-establish health after frustrating standardized therapeutic attempts, unproven interventions in clinical practice with three patients, following §37 of the Declaration of Helsinki, were performed [78]. In the contribution documented here, the results obtained with these three patients are described. The first two received "polyP-hydrogel" supplemented with 600 $\mu$g/mL Na-polyP and 60 $\mu$g/mL "Ca-polyP-NP", while the third one was treated with this "polyP-hydrogel" at the beginning and subsequently for the second lesion also with the polyP-containing collagen-based mats "Ma/Col-Ca-polyP-NP", which were prepared as described previously [27], to cover an exposed tendon.

**Patient 1:** The 90-years old male patient manifested superficial erosions on the right lower leg together with prurigo eczema for 4 mth. Initially, the patient was treated with standardized and modern wound dressings. After an additional 3 mth, only a slight improvement was detected. After that, the wound was treated with "polyP-hydrogel" supplemented with 600 $\mu$g/mL Na-polyP and 60 $\mu$g/mL "Ca-polyP-NP" (a substitution every 3 d). Even after a period of 1 wk, a significant reduction in the wound area was recorded. A complete regeneration was achieved after an additional 7 d.

**Patient 2:** A 55-years old female patient suffered from a ventral ulcer on the tibia for 3 mth. The etiology came from long-term cortisone use due to multiple previous diseases (fibromyalgia, psoriasis arthritis, peripheral arterial occlusive disease, arterial hypertension, migraine, and Darier disease); the latest medication was prednisone (2.5 mg daily) and methotrexate (15 mg weekly). Until admission to the clinics (10.11.), the patient was treated with several gauze dressings. In the clinics, the treatment started with "polyP-hydrogel" containing 600 $\mu$g/mL Na-polyP and 60 $\mu$g/mL "Ca-polyP-NP"; change of the hydrogel every 3 d. After 8 wk of treatment with the hydrogel, the wound area had shrunk by 86.5% and 2 mth later complete (100%) wound closure was achieved, allowing termination of the treatment.

**Patient 3:** The 90-years old male patient suffered from two chronic lesions (ventral and medial) that developed after resection of an ulcerated basal cell carcinoma on the lower leg in October 2021. The postoperative disorders of wound healing occurred together with bacterial infections. After elimination of the infection and due to the size of the wound of 15 cm × 5.5 cm, an initial secondary healing of the wound area was first attempted. After 6 wk of standardized therapy, there was neither sufficient granulation tissue nor a significant reduction in the wound area. In addition, the tendon remained exposed in the medial wound lesion.

After another wound cleaning, using low-contact ultrasound-assisted debridement (Sonoca 185®; Söring, Hamburg; Germany), the ventral wound defect was treated with 3 mL of "polyP-hydrogel" containing 600 $\mu$g/mL Na-polyP and 60 $\mu$g/mL "Ca-polyP-NP" (06.12.). The gel was renewed every 3 d. During the following 39 d (14.01.), the size of the wound decreased by ∼30%. A split-skin graft was applied on the ventral clean and intensively granulated wound to accelerate the epithelization and additionally promote wound closure.

In parallel, the medial lesion was covered with a polyP-containing collagen-based mat "Ma/Col-Ca-polyP-NP", which was supplemented with polyP-hydrogel, and replaced every 3 d.

### 2.13. Histological examination

The biopsies of the wounds were taken and fixed in paraformaldehyde (#4760; Sigma) and then embedded into paraffin wax (#03987; Sigma). From there, ∼5 $\mu$m thick sections were taken and mounted onto glass slides (microscope slides; #XX1007615; Sigma-Millipore) [27]. Subsequently, the slices were deparaffinized, then rehydrated and stained.

For staining the slices with hematoxylin/eosin, Mayer's hematoxylin (#MHS1; Sigma-Aldrich) and eosin Y solution (#HT110280; Sigma-Aldrich) were used. In parallel, the specimens were inspected after immunostaining for CD31 (PECAM-1), which accumulates on the surfaces of endothelial cells, thrombocytes, monocytes, and in granulocytes. The slices were reacted with the CD31 (PECAM-1) monoclonal antibody (#12–0311–82; Invitrogen/Thermo Fisher Scientific). The immunocomplexes were visualized after reaction with an ALP-labelled anti-mouse IgG (GtxMu-004-EALP; Dianova, Hamburg; Germany) and treatment with the substrate-

chromogen PolyDetector AEC HRP kit (Bio SB; Santa Barbara; CA). Factor XIII antigen was stained with a polyclonal antibody (#PA5-16423; Invitrogen/Thermo Fisher Scientific) and subsequently with horseradish peroxidase labelled secondary antibody (SBA-4090–05; Dianova). The immunocomplexes were visualized with the chromogen PolyDetector AEC HRP kit (BioSB; Santa Barbara; CA).

### 2.14. Statistical analysis

The analyses were carried out with SigmaPlot 13.0 (Systat Software, Erkrath; Germany) and the resulting graphs were plotted with the help of GraphPad Prism 7.02 (GraphPad Software, San Diego; CA). At least five replicates were performed for each series. The results are given as mean ± standard deviation. The paired *t*-test was applied to assess the significance of the differences. The *p*-values $< 0.01$ are considered as statistically significant (*).

## 3. Results

### 3.1. Hydrogel wound dressing

The regenerative wound dressing based on cellulose as the structural macromolecule-hydrogel and polyP as the metabolic energy-generating and bacteria-eliminating polymer is straightforward to prepare.

#### 3.1.1. Preparation

The hydrogel was fabricated in a one-pot reaction. Aliquots of 100 mL were prepared from the sterile components 1,2-propandiol and HEC suspended in phosphate buffer and saline at the final concentrations listed under “Materials and Methods”. The gel sample was obtained after heating (121 °C; 1 bar) and termed “hydrogel”. The polyP components, usually 600 $\mu$g/mL Na-polyP and 60 $\mu$g/mL “Ca-polyP-NP” (final concentrations), were added to this solution; this gel suspension is named “polyP-hydrogel”. During the preparation, the gel was processed under sterile conditions. The final pH was adjusted to ~6.5.

Aliquots of 10 mL were packaged into syringes fitted with a Luer Lock adapter and sealing cap (Fig. 2(I-A)).

#### 3.1.2. Surface morphology

If plated onto a glass slide and dried for electron microscopic inspection, the surface of the “hydrogel” samples is wrinkled-flat and interspersed with frost cracks (Fig. 3(I-A, I-B). In contrast, under the same magnification conditions, the hydrogel appears with globular protrusions (Fig. 3(I-D)), which are caused by aggregates of ~100 nm large Ca-polyP-NP (Fig. 3(I-E)). If the surface of the “hydrogel” samples is immersed in DMEM medium/10% FCS for 5 h, and then, after washing in saline, freeze-dried for light microscopic inspection, the area is highlighted only in faintly glossy (Fig. 3(I-C)). In contrast, if the “polyP-hydrogel” is examined, the surface appears brilliant-glossy (Fig. 3(I-F)). As outlined below, this appearance on top of the “polyP-hydrogel” could be attributed to the polyP coacervate.

#### 3.1.3. Mechanical characterization and coacervate formation

If placed onto an inverted glass Petri dish, the hydrogel is viscous and does not form a completely plain surface (Fig. 2(I-A)). If a drop of saline is laid onto the polyP-containing gel with a needle (Fig. 2(I-B)), the solution spreads immediately, forcing the appearance of schlieren after 30 min (Fig. 2(I-C)). Since the pH of the gel is around 6.5, bulky coacervate deposits are formed during a 60 min period from the Na-polyP ingredient within the gel [49] (Fig. 2(I-D)). If the gel sample is overlaid with DMEM medium/10% FCS, not only the soluble Na-polyP but also the particulate “Ca-polyP-NP” transforms into a soluble phase and boosts coacervate formation (Fig. 2(I-E) to Fig. 2(I-G)), which proceeds time-dependently from 60 min (Fig. 2(I-E)), 90 min (Fig. 2(I-F)) to 120 min (Fig. 2(I-G)).

#### 3.1.4. Viscosity

The viscosity of the HEC-based wound gels was determined in a Brookfield/PCE-RVI 1 viscometer at standard concentration conditions of 2% (w/v) HEC. The viscosity as a function of shear speed is shown in Fig. 2(II). The curves show a steep decrease at low shear speed, which levels off at higher velocity. In general, the hydrogel plus polyP (“polyP-hydrogel”; containing 600 $\mu$g/mL Na-polyP and 60 $\mu$g/mL “Ca-polyP-NP”) has a higher viscosity compared to the hydrogel (“hydrogel”) not supplemented with the polymer. The viscosity progression curves for the “polyP-hydrogel” level off at around 25 Pa s, while those for the plain “hydrogel” reach ~20 Pa s (Fig. 2(II)). These values match those given by the manufacturer with 10.8 Pa s for the HEC solution alone (under standard conditions).

A more precise numerical presentation is given in Fig. 2(III). In addition to the differences between the two hydrogel preparations, “polyP-hydrogel” and “hydrogel”, it is remarkable that the viscosities of the hydrogels without polyP are significantly lower in comparison to those with the polymer. Similarly, the viscosity values at 23 °C are markedly higher compared to those found at 37 °C. As an example, at a temperature of 23 °C and a r/min of 12, the “hydrogel” gives a dynamic viscosity of 27.4 Pa s, a value which is statistically different from that measured for the “polyP-hydrogel” with 32.9 Pa s. The corresponding dynamic viscosity values for 37 °C give values of 19.5 Pa s vs 23.4 Pa s (“hydrogel” vs “polyP-hydrogel”).

#### 3.1.5. Circumvallation of bacteria by the *polyP-coacervate*

Overnight samples of *S. aureus* were transferred onto Petri dishes (5 cm) covered with either “hydrogel” or “polyP-hydrogel” and then incubated for 120 min with a TSB medium. In the series with “hydrogel”, the suspension of bacteria does not clump together during the entire incubation period (Fig. 3(II-A, II-B). Very much in contrast, the *S. aureus* bacteria if layered and suspended onto “polyP-hydrogel” start to clump together during coacervate formation and follow the schlieren pattern already during a 60 min incubation period (Fig. 3(II-C, II-D)). The polyP-based coacervate clumps increase with time and increasingly engulf free bacteria in the coacervate (Fig. 3(II-E, II-F)). At higher magnification, it becomes overt that almost all *S. aureus* bacteria are encapsulated in the coacervate clumps (Fig. 3(II-G, II-H)).

### 3.2. Killing of S. aureus

The inhibitory activity of polyP was determined by both the plate inhibition zone assay and the *in vitro* antibacterial activity assay in solution.

#### 3.2.1. Antibacterial activity: plate inhibition zone assay

For qualitative assessment of the polyP-mediated bacterial growth inhibition, the paper disk assay was applied. *S. aureus* was plated onto infusion agar with 10% sheep blood. The polyP samples (20 µL aliquots) were applied onto the filter discs. After an incubation period of 15 h, the diameter of the inhibition zone was measured and the plates were photographed. Under routine conditions and in the absence of additional supplementation with $CaCl_2$, the $Ca^{2+}$ level in the medium/serum is 0.2 mM. The polymer was added in a volume of 20 µL to the 5 mm size paper discs. Under these conditions, the degree of bacterial growth inhibition with Na-polyP is low (Fig. 4(I)); even at a concentration of 600 µg/mL of the polymer, the zone of inhibition increases only marginally from 0 mm (controls) to 0.5 mm. If the agar/serum

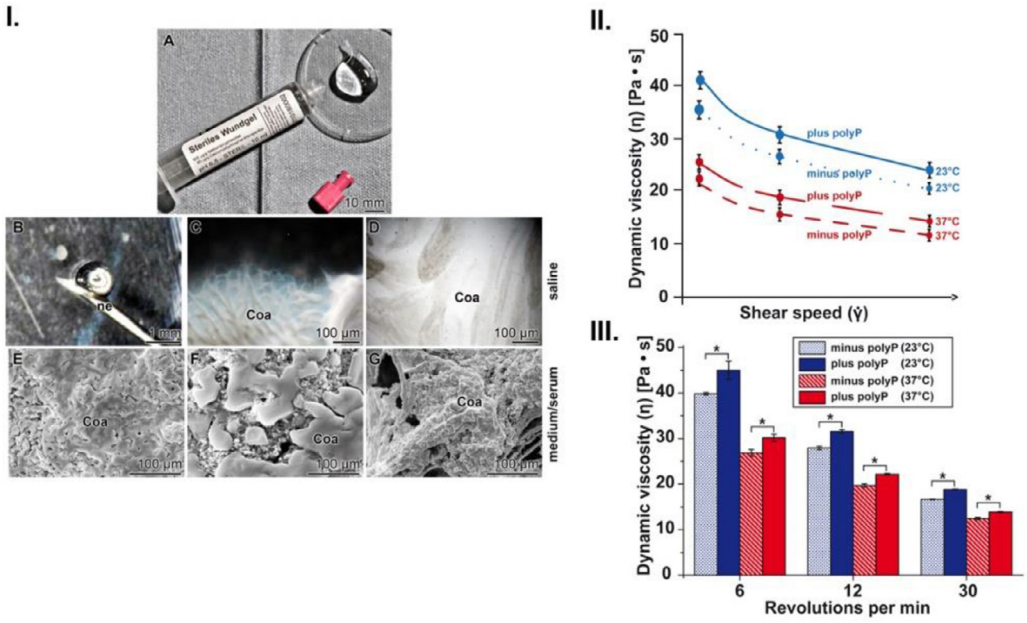


**Fig. 2.** Hydrogel preparation for wound dressing containing both Na-polyP and "Ca-polyP-NP". (I.) (A) The hydrogel is aliquoted in 10 mL samples in syringes. (B–D) Coacervate formation on the surface of the "polyP-hydrogel" supplemented with 600 $\mu$g/mL Na-polyP and 60 $\mu$g/mL "Ca-polyP-NP". If the gel specimens are overlayed with saline *via* a needle (ne), the readily soluble Na-polyP undergoes coacervate (Coa) formation within 30 min; light microscopy. (E)–(G) If the gel is overlayed with medium/serum, both the particulate "Ca-polyP-NP" and the soluble Na-polyP transform into the soluble phase and form coacervate (Coa) droplets; ESEM. Their size increases during a period of 60 min (E), 90 min (F) to 120 min (G). (II.) Determination of the viscosities of the polyP-lacking hydrogel (minus polyP) vs the polymer-containing gel "polyP-hydrogel" (plus polyP) measured at 23 °C (in blue) and at 37 °C (in red). (III.) Numerical presentation of the values for the dynamic viscosity for the gels in the absence of polyP (minus polyP; dashed) in comparison to those from gels supplemented with polyP (solid bars). The determinations were performed at 23 °C (in blue) and at 37 °C (in red). The r/min values for 6, 12, and 30 revolutions are selected. ($n = 5$; $^*p < 0.01$).

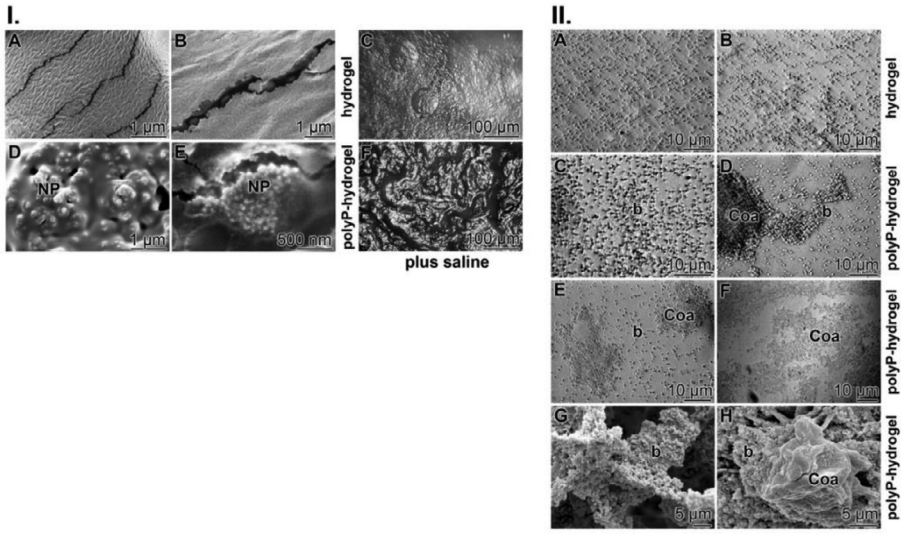


**Fig. 3.** Surface patterns of the hydrogel, "hydrogel", and of the polyP-supplemented "polyP-hydrogel" during coacervate formation and engulfment of bacteria into polyP coacervates. (I.) Surface patterns. (A) and (B) Surface of the "hydrogel" displaying some cracks, which appeared during freeze-drying of the samples; ESEM. (C) Surface of the "hydrogel" after treatment with DMEM/FCS for 5 h; light microscopy. (D) and (E) Surface of the "polyP-hydrogel" with the protruding bulbs, which are caused by the underlying 100 nm large nanoparticles (NP) of "Ca-polyP-NP"; ESEM. (F) The shining surface of "polyP-hydrogel" after incubation for 5 h with DMEM/FCS; light microscopy. (II.) Changes of *S. aureus* suspension on the hydrogels; light microscopy. (A) and (B) The bacteria on the "hydrogel" surface remain suspended during the 120 min incubation in a TSB medium. (C)–(F) Individually suspended *S. aureus* bacteria (b) onto "polyP-hydrogel" undergo step-wise aggregation into the clumps during coacervation (Coa); light microscopy. (G) and (H) At higher magnification, ESEM, it is evident that the individual bacteria (b) are engulfed in the coacervate (Coa) complexes ((C) and (D): 60 min; (E) to (H): 120 min); SEM.

system is supplemented with $CaCl_2$ to 5 mM, the inhibition level increases substantially, especially if Na-polyP is added together with "Ca-polyP-NP". In the combination Na-polyP:"Ca-polyP-NP", 300 µg/mL:30 µg/mL, the inhibition zone already increases to ~2.3 mm. A further increase in the concentration of polyP (Na-polyP:"Ca-polyP-NP") in the 20 µL aliquot applied onto the filter paper to 600 µg/mL:60 µg/mL results in a strong increase of the inhibition zone to ~7 mm.

*3.2.2. Antibacterial activity:* assay in solution

A quantitative determination of the antibacterial activity caused by polyP in the hydrogels was performed in the solution assay. In order to make this feasible, the hydrogels were diluted to 30% with a phosphate buffer. Then, 200 µL of the polyP-free hydrogel or "polyP-hydrogel" [Na-polyP:"Ca-polyP-NP"–600 µg/mL:60 µg/mL] was added to the bacterial suspension supplemented with 5 mM $Ca^{2+}$. The incubation was performed for up to 6 h (Fig. 4(II)). Al-

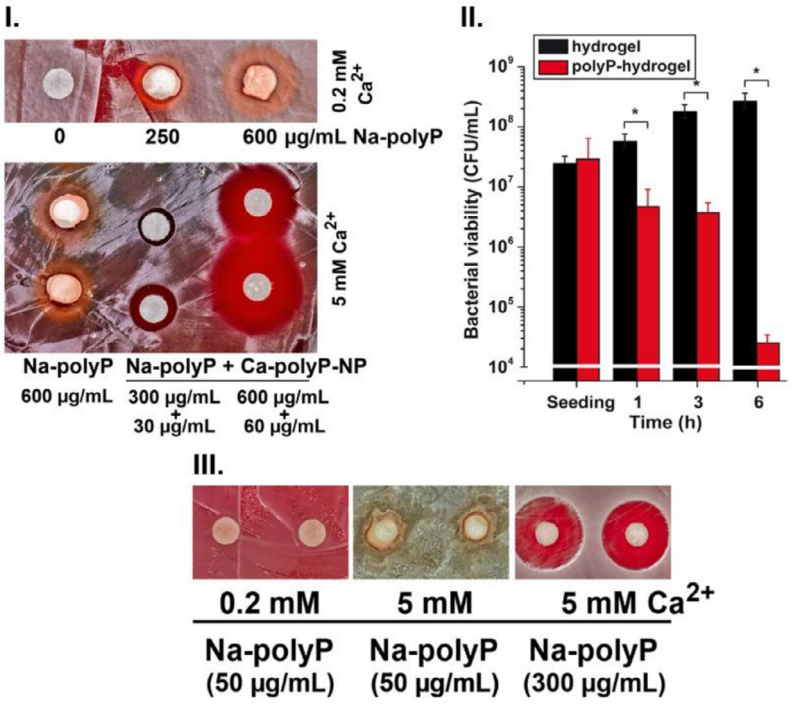


**Fig. 4.** Antibacterial activity of polyP against *S. aureus*. The respective concentrations of polyP are listed. (I.) The inhibitory activity of polyP, either Na-polyP or "Ca-polyP-NP", was tested in the plate inhibition zone assay. In one series (upper row), the inhibition of Na-polyP is determined in medium/serum containing intrinsic 0.2 mM $Ca^{2+}$. In the assays in the lower box, the medium/serum was additionally supplemented with 5 mM $Ca^{2+}$. It is obvious that the degree of inhibition is significantly larger if Na-polyP is enriched with "Ca-polyP-NP". (II.) In parallel, the inhibition of "hydrogel" vs "polyP-hydrogel" is determined in the antibacterial activity assay in solution. Aliquots of *S. aureus* are added to medium/serum supplemented with 5 mM $Ca^{2+}$. The bacterial growth/viability is given in CFU/mL (log scale). (III.) Increase in the inhibitory potency of polyP by addition of $Ca^{2+}$. As indicated, Na-polyP (50 µg/mL, or 300 µg/mL) was added onto the filter disk and incubated on agar covered with a layer of *S. aureus* in the medium containing either 0.2 mM or 5 mM $Ca^{2+}$.

ready after a 1 h period, a significant reduction of the CFU number of polyP-hydrogel treated bacteria was measured (one log10 unit). During the following incubation period (3 h and 6 h), the inhibition increases by 1.5 log10 units and 4 log10 units, respectively (Fig. 4(II)).

*3.2.3. Antibacterial activity:* dependence on $Ca^{2+}$ concentration

As seen in Fig. 4(I), the strength of the antibacterial inhibitory activity caused by polyP is decisively dependent on the $Ca^{2+}$ concentration. This property is directly demonstrated by the inhibition zone assay (Fig. 4(III)). For this series of experiments, the polyP concentration is lowered to 50 µg/mL of Na-polyP in order to strengthen the visible effect. Under conditions of $Ca^{2+}$-non-supplemented medium/serum, no inhibition is seen. However, if the medium/serum is supplemented with 5 mM $Ca^{2+}$, the inhibition zone in the assay with 50 µg/mL of Na-polyP increases to 0.5 mm and with 300 µg/mL even to 8 mm.

*3.3. Effect of polyP on the extracellular ATP level*

Epidermal keratinocytes were chosen for this series of experiments because they represent the major cellular fraction of the epidermis, play critical roles during wound healing, which are dependent on vascularization during wound regeneration [79], and are provided with the enzymatic machinery for ATP generation as well as the receptor-mediated (P2 receptors) metabolic circuits [33].

The keratinocytes were plated onto the "hydrogel" matrix supplemented with different concentrations and compositions of Na-polyP and "Ca-polyP-NP". If the cells were cultured on the "hydrogel" matrix for two days, they form a dense surface layer of cells that are lacking any microvilli (Fig. 5(I-A, I-B)). In contrast, if the cells were cultivated on "polyP-hydrogel" (supplemented with 600 $\mu$g/mL Na-polyP and 60 $\mu$g/mL "Ca-polyP-NP"), the keratinocytes develop a densely covered surface pattern with 1.5 µm long microvilli (Fig. 5(I-C, I-D)), reflecting an intense metabolism of the cells [80] and a marked sensor potential of the cells [81].

Keratinocytes release ATP into the extracellular space, as was initially also reported for bone-like SaOS-2 cells [30, 33]. The distinguishing feature of polyP is that it is a polymer that acts as a generator for metabolic ATP in the extracellular space [37]. In this compartment, ATP also triggers the microvascularization process [21] through chemosensing [25]. The addition of a Na-polyP supplement of 30 µg/mL to 1000 µg/mL to the hydrogel causes a significant increase in the extracellular ATP level from 182 pmol to 335 pmol (per $10^6$ cells); control: 120 pmol (per $10^6$ cells) (Fig. 5(II)). Using the same polyP concentration range, "Ca-polyP-NP" significantly amplifies the extracellular ATP level not only compared to the control but also to Na-polyP. Therefore, the combination of Na-polyP together with "Ca-polyP-NP" was embedded into the hydrogel matrix. The 300 $\mu$g/mL Na-polyP:30 $\mu$g/mL "Ca-polyP-NP" concentration pair causes a further increase in the extracellular level to 745 pmol ($10^6$ cells), significantly higher than with 300 $\mu$g/mL Na-polyP alone (275 pmol in the assays with $10^6$ cells). A slightly but not significantly higher extracellular ATP concentration was seen in assays with 600 $\mu$g/mL Na-polyP:60 $\mu$g/mL "Ca-polyP-NP", which gave 827 pmol ($10^6$ cells).

This polyP-based increase in the extracellular ATP level is almost completely abolished after pre-incubation of the cells with LEV and $Ap_5A$, compounds that abolish the activity of the two key enzymes involved in the polyP generation, ALP and ADK. To clarify if polyP, packed as "Ca-polyP-NP", is also taken up by the cells through clathrin-dependent endocytosis, the cells were pre-incubated with the blocker trifluoperazine (TFP). This active sub-

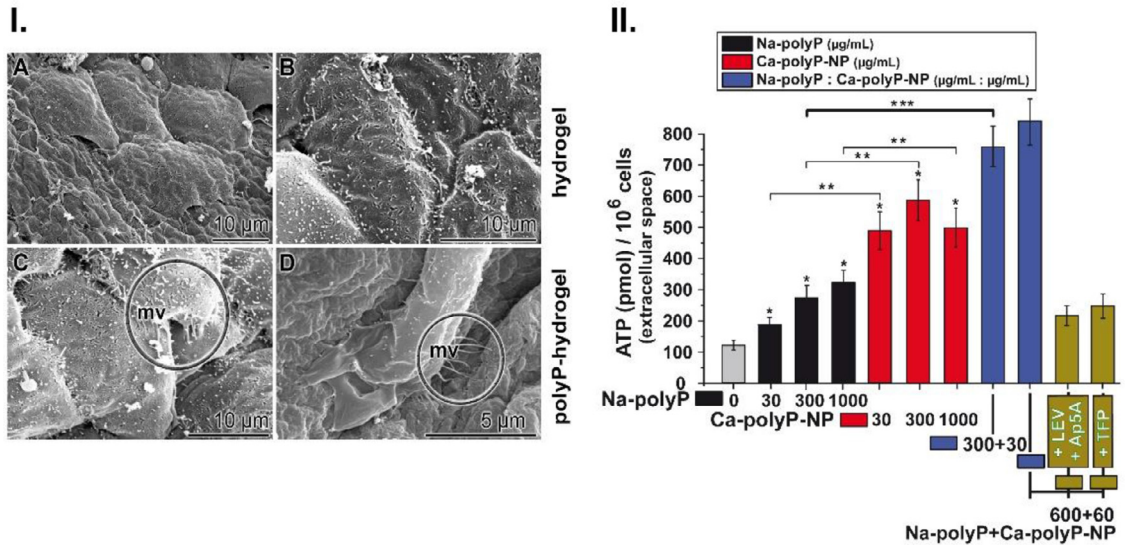


**Fig. 5.** Change of keratinocytes morphology and extracellular ATP level in keratinocyte cultures in response to polyP. (I.) The cells were plated onto (A) and (B) "hydrogel" or onto (C) and (D) "polyP-hydrogel" (containing 600 $\mu$g/mL Na-polyP and 60 $\mu$g/mL "Ca-polyP-NP). On the polyP-containing hydrogel, the keratinocytes develop microvilli (mv). (II.) Extracellular ATP level in keratinocyte cultures, which were plated onto "hydrogel" (0 µg/mL Na-polyP) or onto a hydrogel substrate enriched with 30 to 1000 µg/mL Na-polyP (black bars) or 30 to 1000 µg/mL "Ca-polyP-NP" (red bars). Two concentration pairs of Na-polyP and "Ca-polyP-NP", either 300 $\mu$g/mL Na-polyP plus 30 $\mu$g/mL "Ca-polyP-NP" or 600 $\mu$g/mL Na-polyP plus 60 $\mu$g/mL "Ca-polyP-NP" (blue bars) have been selected. In addition, the cells were pre-incubated with LEV together with $Ap_5A$ (inhibitors of ALP and ADK) or with TFP (blocker of endocytosis) (yellow bars) at concentrations listed under "Materials and Methods". After an incubation of 2 h, the ATP level was determined with the ATP-monitoring luminescence assay. The ATP concentration is given in pmol/$10^6$ viable cells. The values came from five parallel assays and are given as mean ± SD, $^{*}p < 0.01$ for the differences between the controls (absence of polyP) and the polyP supplemented hydrogels; $^{**}p < 0.01$ for the differences between Na-polyP and "Ca-polyP-NP"; and $^{***}p < 0.01$ for difference between a hydrogel with 300 µg/mL Na-polyP alone or in combination with 30 µg/mL "Ca-polyP-NP".

stance reduced the ATP level in the extracellular space by 70%, compared to the assays without TFP (Fig. 5(II)).

### 3.4. Differential effect of *Na-polyP* and "Ca-polyP-NP", separately and in combination

Keratinocytes were grown for 24 h onto either the "hydrogel" matrix or the polyP-supplemented gel "polyP-hydrogel" (Fig. 6(I)). Under otherwise identical conditions, keratinocytes form a patchy-like pattern on the polyP-lacking hydrogel (Fig. 6(I-A)). Addition of a mixture of Na-polyP:"Ca-polyP-NP" at the same 10:1 concentration ratio, increasing from 100 µg/mL Na-polyP:10 µg/mL "Ca-polyP-NP" to 600 µg/mL Na-polyP:60 µg/mL "Ca-polyP-NP" results in a progressive increase in cell density until finally a cobblestone-like morphology is reached (Fig. 6(I-B) to Fig. 6(I-D)).

In parallel, the effect of polyP in the hydrogel on the attachment pattern of epithelial A549 cells was studied. In the absence of the polymer, again a scattered distribution of the cells is visualized. Supplementation of the hydrogel with a mixture Na-polyP:"Ca-polyP-NP", selecting 300 µg/mL Na-polyP:30 µg/mL "Ca-polyP-NP" and 600 µg/mL Na-polyP:60 µg/mL "Ca-polyP-NP", leads to a more dense arrangement of the cells (Fig. 6(II-B, II-C)).

A quantitative analysis of the effect of polyP on the viability/growth of A549 cells was measured with the colorimetric assay PrestoBlue system. If the two polyP formulations were tested separately, no significant effect was measured for both Na-polyP and "Ca-polyP-NP" in the concentration range 300 µg/mL and 1000 µg/mL. However, if a mixture of Na-polyP:"Ca-polyP-NP" is added to the cells, a significant increase in the viability is measured for 300 µg/mL Na-polyP:30 µg/mL and also 600 µg/mL Na-polyP:60 µg/mL by ~25% (Fig. 6(III)).

### 3.5. Application of polyP-containing hydrogel for chronic wounds

Of the three patients who were enrolled and treated continuously with "polyP-hydrogel", all showed a significant reduction in wound size and finally complete healing of their respective wounds. The study was conducted as individual treatments. In the present article, two patients are described who exclusively received "polyP-hydrogel" supplemented with 600 $\mu$g/mL Na-polyP and 60 $\mu$g/mL "Ca-polyP-NP", while the third patient was treated with this "polyP-hydrogel" at the beginning and subsequently, at the end, for the second lesion also with the polyP-containing collagen-based mats, "Ma/Col-Ca-polyP-NP" [27].

#### 3.5.1. Patient 1—treated exclusively with "polyP-hydrogel"

The 90-years old male patient suffered from superficial erosions for 4 mth. At the first visit, therapy was started with standard dressings for 3 mth (Fig. 7(I)). Since only a marginal improvement occurred, the treatment with "polyP-hydrogel" (with 600 $\mu$g/mL Na-polyP and 60 $\mu$g/mL "Ca-polyP-NP") was initiated (Fig. 7(I-A)). A sample of 3 mL was applied to the surface of the wound and covered with neutral gauze (Fig. 7(I-B)). Every 3 d the gel was renewed. Even after 1 wk of treatment, the wound size was found to be reduced to 19.5% of the initial extent (Fig. 7(I-C)). A complete wound closure with complete epithelization was reached after an additional week (Fig. 7(I-D)).

#### 3.5.2. Patient 2—treated with "polyP-hydrogel" only

The 55-years old female patient showed for 3 mth a ventral ulcer on the tibia after surgical intervention (Fig. 7(II)). In addition, she was on long-term steroid therapy due to rheumatic disease. Previous attempts at therapy have been frustrating. The treatment with "polyP-hydrogel" (containing 600 $\mu$g/mL Na-polyP and 60 $\mu$g/mL "Ca-polyP-NP") was started (Fig. 7(II-A)). The response of the patient was very significant. After 2 mth of therapy, the wound size reduced to 13.5% of the initial size (Fig. 7(II-B)). In the following 8 wk, the dimension of the wound reduced almost completely so that further treatment was no longer indicated (Fig. 7(II-C)).

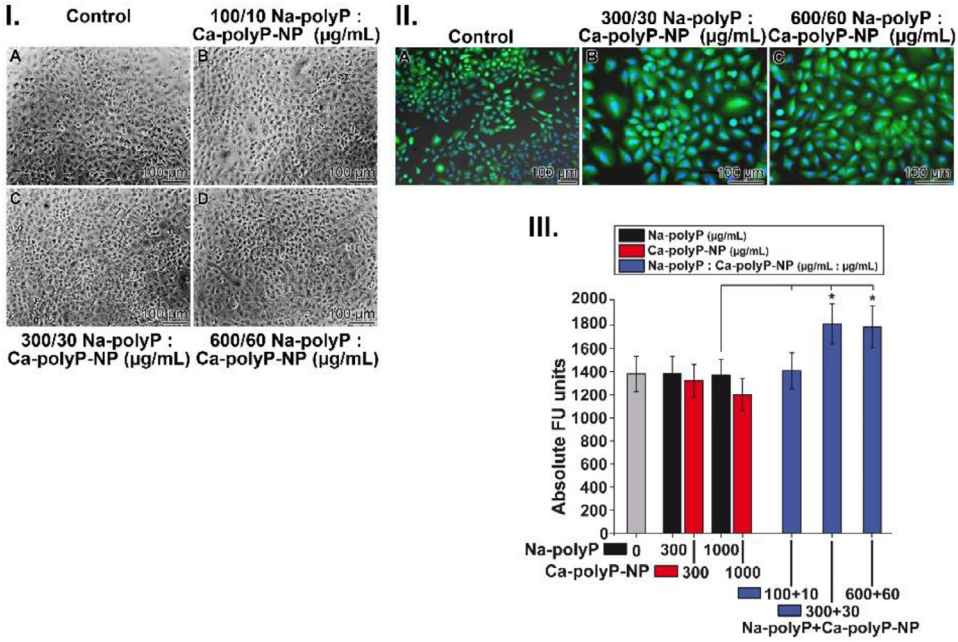


**Fig. 6.** Effect of polyP on both cell attachment and viability/growth of keratinocytes and epithelial A549 cells; the incubation time was 24 h. (I.) Keratinocytes were seeded onto control hydrogel and hydrogel supplemented with a mixture of Na-polyP and "Ca-polyP-NP"; a 10:1 concentration ratio between these two polyP formulations has been selected. In contrast to the pattern on the polyP-free gel, the polymer-supplemented hydrogels allow an increase in cell density and a formation of a cobblestone-like arrangement pattern; Nomarski phase contrast microscopy. (II.) A similar experimental arrangement was performed with A549 cells. Also in this system, the mixture of Na-polyP:"Ca-polyP-NP" causes an increased cell density. The cells are stained with Calcein-AM; fluorescence microscopy. (III.) Determination of the viability/growth of A549 cells using the PrestoBlue system. The results are given in absolute fluorescence units in dependence on polyP concentration. The polymer is added either individually as Na-polyP (black bars) or as "Ca-polyP-NP" (red bars). In addition, the two formulations are added in a 10:1 mixture to the cells (blue bars). Ten parallel experiments were performed; the data given are means ± SD ($^*p < 0.01$).

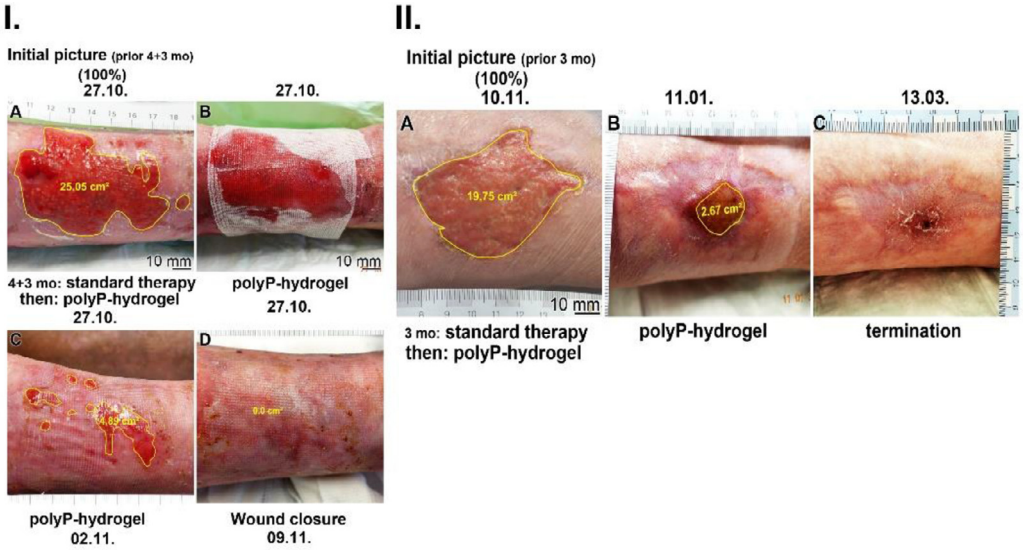


**Fig. 7.** Accelerating effect of "polyP-hydrogel" (with 600 $\mu$g/mL Na-polyP and 60 $\mu$g/mL "Ca-polyP-NP") on the healing process of chronic wounds. (I.) First patient. He received on (A) the initial, pre-treated wound the "polyP-hydrogel", which was covered with (B) neutral gauze. (C) and (D) During treatment with this hydrogel, the wound area was reduced to 19.5% of the initial size or even completely. (II.) A second patient was treated similarly. Starting from (A) a large, again pre-treated wound *via* (B) a 2 mth therapy with the "polyP-hydrogel", (C) a healing step was reached, which allowed termination of treatment.

*3.5.3.* Patient 3—treated with "polyP-hydrogel" and *polyP*-containing collagen-based mats "Ma/Col-Ca-polyP-NP"

The male patient was 95 years old. He suffered from two chronic wounds in the lower leg, which developed after resection of ulcerated basal cell carcinoma. Both wounds were infected and had to be cleaned and conditioned first. With the help of ultrasound-assisted wound debridement, an improvement of the wound condition could be achieved (Fig. 8). The lesions emerged on the ventral side (Fig. 8(A-1)) and the medial side (Fig. 8(B-1)) of the leg.

To further promote wound healing and achieve wound closure, "polyP-hydrogel" was applied to the ventral defect (Fig. 8(A)), and a polyP-containing collagen-based mat "Ma/Col-Ca-polyP-NP" was applied to the medial wound (Fig. 8(B)). The treatment of the latter, medial, wound was necessary because there a tendon was exposed. The ventral wound was treated with 3 mL "polyP-hydrogel"

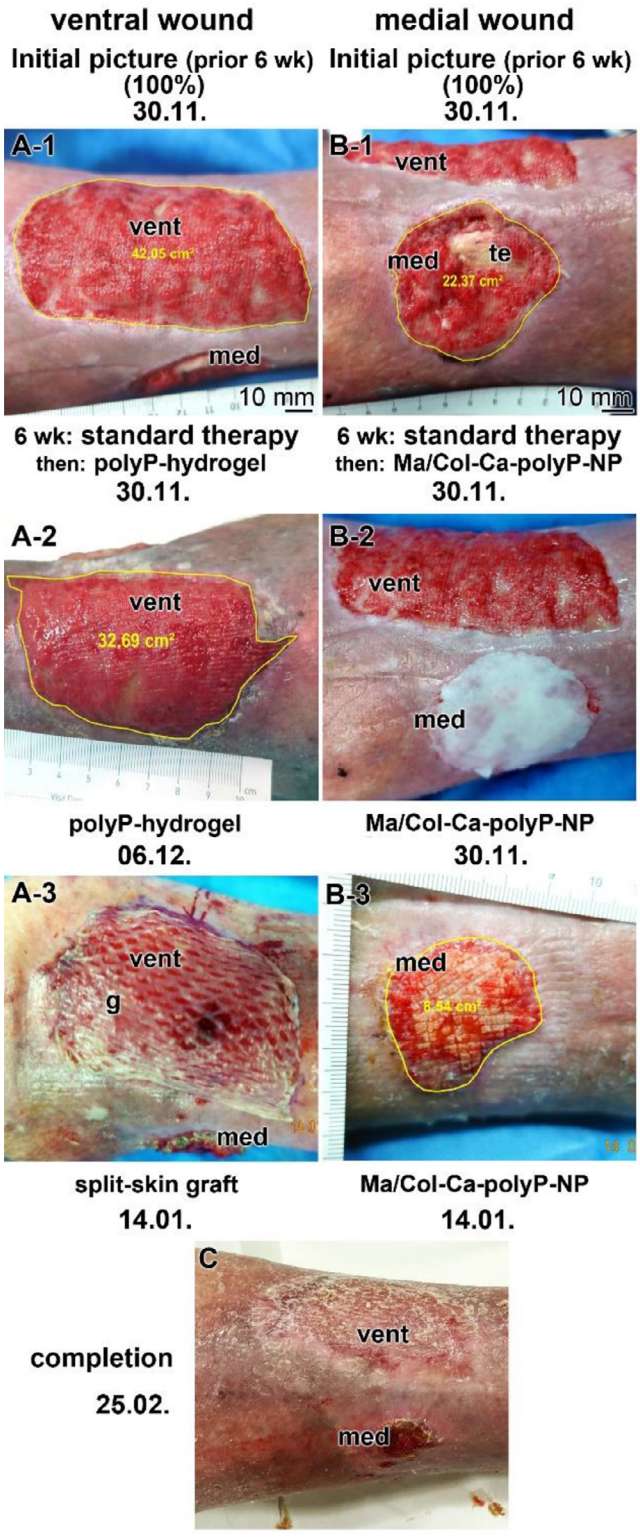


**Fig. 8.** This patient (third Patient) developed two chronic wounds at the lower leg after surgical removal of an ulcerated basal cell carcinoma located either ventrally (A row) or medially (B row). The wound was pretreated with paraffin gauze for 6 wk. Subsequently, (A-1)–(A-3) the larger ventral wound was treated (A-1) and (A-2) first with "polyP-hydrogel" and after a reduction of the wound to less than 20% and a stabilization of the wound (A-2) during treatment, the wound was suitable for (A-3) transplantation with a split-skin graft (g). In parallel, the smaller, medial wound (B-1), which exposed the internal tendon (te), was covered with (B-2) a polyP-containing collagen-based mat "Ma/Col-Ca-polyP-NP" through which a reduction of the wound occurred. (B-3) The mat integrated into the regenerating wound. (C) In the course of the 6 wk treatment of the wounds with either (A row) the "polyP-hydrogel"/split-skin graft or (B row) the "Ma/Col-Ca-polyP-NP", the two wounds healed completely, both almost to the same extent.

(600 $\mu$g/mL Na-polyP and 60 $\mu$g/mL "Ca-polyP-NP"), which was replaced every 3 d (Fig. 8(A-2)). After 6 wk, the wound area was reduced by almost 30% with stable and effective granulation tissue, allowing transplantation with a split-skin graft to shorten the epithelization process (Fig. 8(A-3)).

In parallel, the medial wound, with the exposed tendon (Fig. 8(B-1)), which was covered with polyP-containing collagen-based mats "Ma/Col-Ca-polyP-NP" (Fig. 8(B-2)), and additionally treated with "polyP-hydrogel", shows a complete integration of the mat with sufficient coverage of the tendon and a reduction of the wound area by more than 60% (Fig. 8 (B-1) vs Fig. 8(B-3)). The latter image also shows that the mat became integrated as a structural element into the regenerating granulation tissue. Due to the small wound area, no skin transplantation was necessary.

Complete wound closure of both defects was achieved simultaneously after a total of 16 wk (Fig. 8(C)).

### *3.6. Increased granulation of the chronic wounds after their coverage with polyP-supplemented mats and hydrogel*

The formation/development of granulation tissue within a wound is a characteristic sign of progression from the inflammatory phase to the healing reconstitution phase [82]. In turn, histological sections were prepared from Patient 3. The two chronical wounds were treated with different regimens. The ventral wound was covered first with "polyP-hydrogel" and in the final regeneration phase with a split-skin graft (Fig. 8(A)). In parallel, the medial wound was treated with a "Ma/Col-Ca-polyP-NP" mat (Fig. 8(B)). Both schedules resulted in complete healing of the lesions (Fig. 8(C)). The "polyP-hydrogel" has the advantage that it imitates the physiological skin environment with respect to the porous and hydrated molecular structure and covers most tightly the lesion. In contrast, the mats ("Ma/Col-Ca-polyP-NP") require a longer replacement period and sufficient coverage of exposed vital structures for stabilization. It is up to the treating physician to decide which strategy is best to choose.

The histological analyses were performed firstly with hematoxylin/eosin-stained biopsy slices and secondly with antibodies to visualize the vascularization state. The hematoxylin/eosin images show that during the 3 d period (change of the hydrogel), the hydrogel coverage disappears and becomes integrated into the regenerated tissue (Fig. 9(I-A)). The underlying tissue is in the repair phase, as can be monitored after a 6 wk period. The granulation tissue is already structured and comprises numerous microvessels (Fig. 9(I-B)). In comparison, beneath the collagen mats, the regenerating granulation tissue is traversed by fibroblast bundles that penetrate into the regenerating endothelial cell layers (Fig. 9(I-C, I-D)) already 4 wk after overlaying with the "Ma/Col-Ca-polyP-NP" mats. This cell organization increases further and additionally shows embedded microvessels (Fig. 9(I-E, I-F)) after 6 wk.

A contrasted hematoxylin/eosin staining of the slices demonstrates that the cells in the granulation zone of the regenerating wound in wounds treated with "polyP-hydrogel" are interspersed with microvessels after 6 wk (Fig. 9(II-A)), which are surrounded by cells irregularly organized to bundles. After the same period of treatment using "Ma/Col-Ca-polyP-NP" mats, the diameter of the vessels increases significantly. They are nestled into organized cell clusters (Fig. 9(II-B)). Reacting the slices with Factor XIII antibodies, which stain blood platelets and fibroblast-like mesenchymal cells [83], highlights those cells, which are arranged in bundles (Fig. 9(II-C)). The application of a CD31 antibody highlights the vessels both in regenerating tissue treated for 6 wk with "polyP-hydrogel" (Fig. 9(II-D)) or with "Ma/Col-Ca-polyP-NP" mats (Fig. 9(II-E)). In comparison, the abundance of the vessels in the "Ma/Col-Ca-polyP-NP" series is strikingly higher.

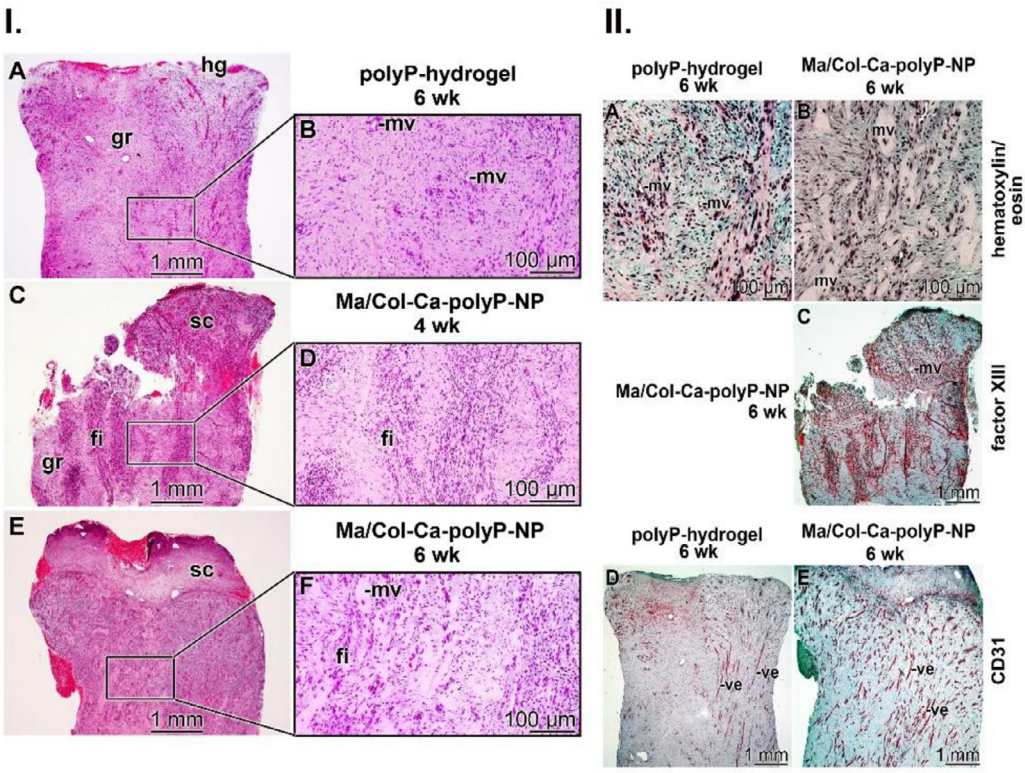


**Fig. 9.** The effect of treatment of the chronic wounds of Patient 3 with either "polyP-hydrogel" or with "Ma/Col-Ca-polyP-NP" mats. (I.) Staining of biopsy slices with hematoxylin/eosin. The hydrogel (hg) coverage and wound scab (sc) are marked. The slices were obtained from biopsies taken 4 wk or 6 wk from the tissue samples on the regenerating wound, which was treated with either "polyP-hydrogel" or with "Ma/Col-Ca-polyP-NP" mats as indicated (A, C, E). Some microvessels (mv) and fibroblast bundles (fi), as well as granulation tissue units (gr), are marked. Characteristic areas are marked (square) and given in higher magnifications (B, D, F). (II.) Biopsy slices from wound areas, treated with either "polyP-hydrogel" or with "Ma/Col-Ca-polyP-NP" mats, after a 6 wk treatment, were stained with (A) and (B) hematoxylin/eosin or reacted with antibodies against (C) factor XIII or (D and E) the CD31 antigen for immune-histology. Some microvessels (mv) or larger blood microvessels (ve) are marked.

In addition, the slices show that the cells in the regenerated area from wounds treated with "Ma/Col-Ca-polyP-NP" mats rather than "polyP-hydrogel" show a slightly higher histological order/more accurate architecture. This effect is most likely the result of the higher organization of the vessels due to the collagen fiber arrangement present in the mats (Fig. 9(II-B) vs Fig. 9(II-A)). With the healing time, the maturation of the scar in the "Ma/Col-Ca-polyP-NP" mats continues and the arrangement of cells shows a transient yet random pattern (Fig. 9(II-C)), and after 6 wk of treatment a well-arranged orientation of the longitudinally aligned growing vessels (Fig. 9(II-E)).

## 4. Discussion

Oxygen is a key factor that controls and guides wound regeneration in all phases of wound healing [84]. During the inflammatory phase, oxygen acts as a signal for the directed migration of fibroblasts and contributes to the antibacterial activity of leukocytes (myeloid cells or lymphoid cells). During the proliferative phase, oxygen sensing initiates angiogenesis by activating endothelial and smooth muscle cells. In addition, oxygen is needed for the production of collagen during the remodeling stage. Under normoxic conditions, oxygen drives the mitochondrial cytochrome oxidase, thereby enabling the production of high-energy phosphates, mainly ATP [85].

Primary wound healing is an uncomplicated regenerative process of non-infected wounds. During the management of secondary wound healing, it is important to ensure that the injury remains moist in the physiological environment. Air promotes dehydration and can lead to extensive, often irreparable tissue necrosis. These "physiological" wound healing processes must be distinguished from those that are complicated by underlying pathologies such as diabetes mellitus [86], chronic venous/arterial insufficiency, and immunological or dermatological diseases [87]. In both situations, extreme hypoxia leads to cellular death. In the mitochondria, oxygen feeds oxidative phosphorylation, ultimately allowing the $F_1F_O$-ATP synthase, which is embedded in the mitochondrial inner membrane and produces the bulk of the cellular ATP [88], to deliver metabolic energy for intermediary metabolism. During mitochondrial respiration, which produces 30–32 molecules of ATP per molecule of glucose, glycolysis alone contributes 2 ATP molecules per glucose molecule. These energy-rich cytoplasmic ATP molecules are signals for the extracellular autocrine sensing mechanism to build microvascularization [23].

The ATP level in the extracellular space is low. However, the newly described extracellular generator of ATP, polyP, increases this pool *via* enzymatic breakdown of the polymer [37]. PolyP is released during the activation of the blood platelets [89]. At any site in the body, where damage occurs, the platelets accumulate and accelerate the healing of the injury [90]. Only recently was it established that polyP in eukaryotes acts as a rich source for the generation of metabolic energy [30], as it is also known for bacteria [91]. This discovery opens a new avenue in regenerative medicine, from soft/hard tissue repair to human wound healing [26,27]. The effectiveness of polyP as a physiological polymer allowing rapid wound healing was proven in mice, even diabetic mice, and now in humans as well.

Previously, we have shown that polyP in the form of a zinc salt, as NP, supports the growth and migration of epidermal keratinocytes, suggesting that such Zn-polyP-NP are also promising

for wound regeneration *in vivo* [92]. However, we subsequently realized that this formulation shows delayed release kinetics, which prompted us to apply Ca-polyP-NP instead [92]. It has also been reported that the application of intracellular ATP delivery results in enhanced wound healing in rabbits. The data presented look very promising [93]. Confirmation of the human situation awaits further reports. In our attempt, the polymer was applied either together with a collagen mat [27] or as a hydrogel (the present study). Another difference to the approach [93] is that in our approach presented here, polyP is administered extracellularly, which is also the site, where polyP is discharged from blood platelets.

ATP has been shown to be present in low concentrations in the extracellular space, where it acts in concert with the other purine nucleotides on the ionotropic (P2X) and the metabotropic (P2Y) receptors [94]. These signaling systems modulate the currents in sensory neurons and also initiate pain, which is associated with muscle ischemia. However, none of these adverse reactions have been observed in animal or human applications.

In the preceding report, polyP has been incorporated into collagen mats, allowing application to wounds with strong barrier properties [27]. To prevent drying out of the wound/wound covering of the regenerating tissue, a moisturizing solution was applied to the wound every 2 to 3 d that was also supplemented with polyP (300 $\mu$g/g Na-polyP; 30 $\mu$g/g "Ca-polyP-NP"). Therefore, we now describe a hydrogel formulation based on hydroxyethyl cellulose (HEC). Here this FDA-approved polymer was used at the established concentration of 2% (w/v). This hydrogel has a dynamic viscosity suitable to provide full coverage of the wound area and is strong enough to overlay the region with a fatty gauze and an adhesive plaster. The pH values in both the mats and the hydrogel remained neutral (pH range 6–7.5) due to the addition of a phosphate buffer during the preparation and the addition of 1,2-propandiol which is known to keep the solution in the neutral range. Likewise, the pH remains neutral at the end of a 3 d application.

The polyP hydrogel formulation supplemented with polyP (termed "polyP-hydrogel") functions due to two unique properties. First, polyP undergoes coacervation, a process in which an aqueous polymer solution separates into two immiscible liquid phases, a dense coacervate phase and a dilute equilibrium phase [95]. This two-liquid-phase system implements two beneficial properties that support wound healing. Coacervates have been shown to provide the eukaryotic cells with a suitable fluid environment for adaptive migration and oriented cell-cell interaction [49]. In addition, the coacervate droplets gradually coalesce, ripen, and finally enclose bacteria and allow polyP to chelate the outer membrane of the microorganisms (Fig. 10(A)). As shown experimentally in the present article, Na-polyP—surely in the coacervate phase—disintegrate the surface organization of the bacterial membrane. As a result, the polyP coacervate inhibits the growth of the bacteria, followed by bacterial death and the survival of viable wound cells. In the *in vitro* studies with polyP, the medium/serum was supplemented with $Ca^{2+}$ (5 mM), since polyP (applied as Na-polyP) would chelate $Ca^{2+}$ in the environment of the bacteria and the bacterial cell walls are sensitive to $Ca^{2+}$ deprivation [96].

Then, secondly, polyP acts as an energy-carrying molecule and, with the two enzymes ALP and ADK, as a generator and transformer of metabolic energy to ATP [37]. In principle, the level of ALP in the bone is higher than in the skin (reviewed in Ref. [37]). However, the activity of ALP in the wound exudate increases sharply, especially during the first 5 d of damage [97,98]. The enzyme does not only originate from the eukaryotic cells but also from the bacteria that accumulate in wounds during the initial phase [99]. Metabolic energy in general and ATP in particular drive the most active cellular processes and certainly also regeneration during wound healing [34]. In addition to the closely interlocked

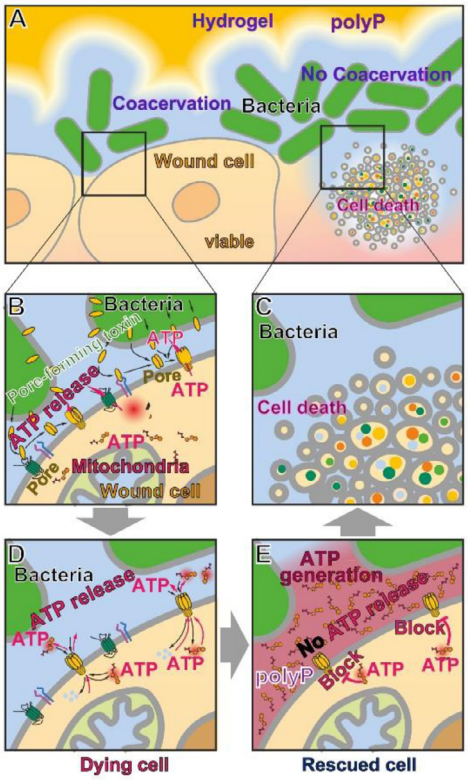


**Fig. 10.** Dual effect of hydrogel-embedded polyP on wound cell survival (scheme). (A) PolyP embedded in the hydrogel is released into the extracellular space where the polymer forms a coacervate. This coacervate enwraps and kills the bacteria. This keeps wound cells viable. In the absence of the polyP-based coacervate, the bacteria cause wound cell death. (B) The bacteria release pore-forming $\alpha$-hemolysins, which become inserted into wound cells. ATP is released from the cells through these pores, resulting in cell death (C). (D) This efflux of ATP through the bacterial pores inserted into the wound cell membranes can be blocked by polyP. (E) ATP generated from polyP in the extracellular space breaks down the internal/external ATP gradient and blocks the release of ATP. The cells are rescued.

metabolic pathways, glycolysis and the coupled mitochondrial respiratory system [100] balance the ATP/ADP ratio and thus the intracellular ATP levels. Furthermore, ATP is the key component in two autocrine signaling mechanisms, a first in which wound-mediated release of endogenous ATP activates $P2Y_2$ receptors to facilitate wound closure [101] and a second in which ATP, generated during glycolysis from glucose and also released into the extracellular space, forms a chemotactic signal to initiate neovascularization [21]. In wound healing, ATP has a prominent function as it counterbalances the release of ATP from fibroblasts and macrophages due to the action of $\alpha$-toxin (hemolysin A, Hla). The $\alpha$-toxin released from pore-forming bacteria is inserted into wound cells [102]; a reverse reaction of hemolysin into the bacterial wall is not known (Fig. 10(B)).

A cellular deprivation of ATP causes cell death *via* apoptosis or necrosis [103] (Fig. 10(C)). Exposure of cells with polyP results in an increase in both the intracellular and extracellular ATP levels [20, 31]. PolyP, especially if delivered as polyP-NP, is taken up by the cells and correlates there with the ATP level. Using transmission electron microscopic analysis, it could be demonstrated that the polyP-nanoparticles are transported into cells, a process that is inhibited by TFP, a clathrin-dependent endocytosis blocker [71]. In turn, we conclude that ATP generated enzymatically from polyP balances the local decrease of ATP around the $\alpha$-hemolysin pores and allows Mg-ATP, having no net charge [104], to pass through the pores in a diffusion-controlled manner [105] (Fig. 10(D)). This bacterial caused release of cellular ATP through the $\alpha$-hemolysin

pores can be blocked by increasing the polyP-mediated ATP levels in the extracellular space, leading to a rescue effect of the wound cells exposing $\alpha$-hemolysin pores (Fig. 10(E)).

PolyP has been demonstrated not only to increase cell growth and survival but also to stimulate the motility of eukaryotic cells in general and keratinocytes in particular [106–108]. Experiments showed that the central point of action during cell cycle progression is the S-phase [109]. Here we showed that, besides human lung epithelial A549 cells, keratinocytes show an increased proliferation with the wound hydrogel used here, supplemented with 300 µg/mL:30 µg/mL or 600 µg/mL:60 µg/mL Na-polyP and "Ca-polyP-NP". The finding that the addition of nanoparticulate Ca-polyP to Na-polyP greatly increases the proliferation capacity of the cells is remarkable. This finding is based on the observation that Na-polyP and "Ca-polyP-NP" have different release kinetics; at first, Na-polyP is enzymatically cleaved in the medium/serum, followed by the enzymatic attack of "Ca-polyP-NP" [50]. In addition, this "synergistic" stimulation of cell growth is due to cellular uptake of the particulate polyP-NP and the subsequent increase in cellular ATP production. Furthermore, we found that exposure of keratinocytes to polyP leads to a marked formation of microvilli. These organelles function as sensors for the cells to their environment but also are involved in the organization of tissue layers through the cell-cell transfer of cell organelles, as shown for melanosomes, which are translocated from melanocytes to keratinocytes [110].

With the two wound dressings (hydrogel and mats) with polyP presented here, several essential goals for successful wound healing are achieved. Firstly, the wounds maintain a moist wound environment; with the mat series, a sterile wetting solution (30 µg/mL of "Ca-polyP-NP") is applied every 3 d—and with the hydrogel series, the moisture originates from the gel. Both coverages contain polyP in ionized form as Na-polyP and as particulate Ca-polyP nanoparticles; the latter type of formulation acts as a depot form [50]. Secondly, the polyP-based wound dressing has an antibacterial effect.

In view of these properties of polyP, the successful application of the two wound coverages for the treatment of chronic wounds was predictable. The healing period was drastically shortened. The histological analyses showed that the healing is based on a physiological reconstitution of the damaged skin area. After a marked granulation of the regenerated area, increasing vascularization was detected, followed by the development of a functional extracellular matrix system. Comparing the reconstitution effect between "polyP-hydrogel" treated and "Ma/Col-Ca-polyP-NP" mats treated wounds, it became overt that the collagen mats promote the direction of the structural elements and of the wound vessels due to an alignment of the cells/fibers along the collagen fibers of the mats. As the polyP-based coverages also address the key cost drivers for chronic wounds by accelerating wound healing, reducing the frequency of visits by health care professionals, and, it appears, by decreasing also the incidence of complications [111] the new approach has the potential to become routine in the clinics and therefore clinical trials are strongly recommended.

## 5. Conclusion

As an outlook, wound research faces eminent challenges due to the multidimensional and multifactorial nature of healing, difficulties in creating appropriate preclinical models, economic burden, duration, and exclusivity of studies [112]. Among the most important steps towards improving wound research and sustainable therapy is—besides the selection of appropriate models for preclinical studies—the availability of suitable standardization criteria. The present work aims to contribute to a solution. It is demonstrated that polyP as a source for the generation of extracellular ATP is an essential contributor to the activation of wound cell metabolism as well as the energy-dependent extracellular organization of the fibrillar network [37]. The extracellular organized scaffold is a basis for the complex process of wound healing, which involves a series of cell types including keratinocytes, macrophages, platelets, fibroblasts, and endothelial cells. The keratinocytes provide pro-inflammatory signals that initially indicate skin damage [113]. In parallel with boosting the clotting cascade and reinforcing hemostasis, the platelets become activated, cells that release growth factors such as the epidermal growth factor, the platelet-derived growth factor, and the transforming growth factor (TGF-$\beta$). And, importantly, they release polyP into the extracellular space [19]. In this compartment, ATP is formed enzymatically from polyP, as shown in the present study. This nucleotide provides the stimulus and the energy for stimulating macrophages to release chemokines such as the macrophage inflammatory protein-2 [114], resulting in the promotion of neutrophil migration. Finally, inflammatory cells remove cell debris and bacteria from the wound site [115]. This latter process and the second effect of polyP are again intensified by polyP/ATP *via* the action of polyP on surrounding bacteria after the transition of the polymer to the coacervate phase. Even more so, the increase in ATP level blocks the function of the bacterial $\alpha$-hemolysin, as shown here. As a result, granulation tissue develops in human chronic wounds, which allows the formation of new vessels, tiny vessels surrounded by fibrin cuffs. Based on these data, it seems advisable to include polyP into a wound dressing to exploit the regenerative potential of this physiological polymer.

## Data availability statement

The data that support the findings of this study are available from the corresponding author upon reasonable request.

## Declaration of Competing Interest

The authors declare no conflict of interest.

## Acknowledgments

We are very much grateful to Dr. Beate Weidenthaler-Barth (Department of Dermatology, University Clinic Mainz) for the very expert histological analyses and the permission to include the images in this study. Moreover, we thank Mrs. Kerstin Bahr, Institute of Functional and Clinical Anatomy, University Medical Center, Mainz (Germany) for her continuous support. In addition, we are thankful to Mrs. Franziska S. Kranz (Medical Center of the Johannes Gutenberg University, Mainz) for her important support. W.E.G. Müller is the holder of an ERC Advanced Investigator Grant (Grant No. 268476). In addition, W.E.G. Müller has obtained three ERC-PoC grants (Si-Bone-PoC, Grant No. 324564; MorphoVES-PoC, Grant No. 662486; and ArthroDUR, Grant No. 767234). In addition, this work was supported by grants from the European Commission (Grant Nos. 604036 and 311848), the International Human Frontier Science Program, and the BiomaTiCS research initiative of the University Medical Center, Mainz. Further support came from the BMBF (Grant No. 13GW0403A/B – SKIN-ENERGY), the BMWi (Grant No. ZF4294002AP9), and the China National Key R & D Plan: China-German Cooperation (Grant No. 2018YFE0194300).

## References

[1] M. Kruse, S.P. Leys, I.M. Müller, W.E.G. Müller, J. Mol. Evol. 46 (1998) 721–728.
[2] C.J. van Koppen, R.W. Hartmann, Expert Opin. Ther. Patents 25 (2015) 931–937.
[3] E.M. Golebiewska, A.W. Poole, Blood Rev. 29 (2015) 153–162.

[4] F. Müller, N.J. Mutch, W.A. Schenk, S.A. Smith, L. Esterl, H.M. Spronk, S. Schmidbauer, W.A. Gahl, J.H. Morrissey, T. Renné, Cell 139 (2009) 1143–1156.
[5] L. Liebermann, Arch. Gesamte Physiol. Menschen Tiere 47 (1890) 155–160.
[6] A. Meyer, Botany 62 (1904) 113–153.
[7] P. Langen, E. Liss, K. Lohmann, in: Acides Ribonucléiques Et Polyphosphates: Structure, Synthèse Et Fonctions: Colloques internationaux Du Centre National De La Recherche Scientifique, Editions du Centre National de la Recherche Scientifique, Paris, France, 1962, pp. 604–614. No. 105.
[8] A. Kornberg, S.R. Kornberg, E.S. Simms, Biochim. Biophys. Acta 20 (1956) 215–227.
[9] I.S. Kulaev, A.N. Belozerskij, Proc. Acad. Sci. USSR 120 (1958) 128–131.
[10] I.S. Kulaev, V. Vagabov, T. Kulakovskaya, The Biochemistry of Inorganic Polyphosphates, 2nd ed., John Wiley, Chichester, United Kingdom, 2004.
[11] B. Lorenz, W.E.G. Müller, I.S. Kulaev, H.C. Schröder, J. Biol. Chem. 269 (1994) 22198–22204.
[12] W.E.G. Müller, S.I. Belikov, W. Tremel, C.C. Perry, W.W.C. Gieskes, A. Boreiko, H.C. Schröder, Micron 37 (2006) 107–120.
[13] H.C. Schröder, W.E.G. Müller, Inorganic Polyphosphates; Biochemistry, Biology, Biotechnology, Progress in Molecular and Subcellular Biology, 23, Springer Verlag, Berlin, Germany, 1999.
[14] R. Docampo, S.N. Moreno, Cell Calcium 50 (2011) 113–119.
[15] W.E.G. Müller, E. Tolba, H.C. Schröder, S.F. Wang, G. Glaßer, R. Muñoz-Espí, T. Link, X.H. Wang, Mater. Lett. 148 (2015) 163–166.
[16] Y. Shanjani, J.N. De Croos, R.M. Pilliar, R.A. Kandel, E. Toyserkani, J. Biomed. Mater. Res. Part B-Appl. Biomater. 93 (2010) 510–519.
[17] S.N. Moreno, R. Docampo, PLoS Pathog. 9 (2013) e1003230.
[18] T.L. Lindahl, S. Ramström, N. Boknäs, L. Faxälv, Biochem. Soc. Trans. 44 (2016) 35–39.
[19] J.I. Weitz, J.C. Fredenburgh, Blood 129 (2017) 1574–1575.
[20] W.E.G. Müller, S.F. Wang, M. Wiens, M. Neufurth, M. Ackermann, D. Relkovic, M. Kokkinopoulou, Q.L. Feng, H.C. Schröder, X.H. Wang, PLoS One 12 (2017) e0188977.
[21] W.E.G. Müller, M. Ackermann, E. Tolba, M. Neufurth, I. Ivetac, M. Kokkinopoulou, H.C. Schröder, X.H. Wang, Biochem. J. 475 (2018) 3255–3273.
[22] G. Leyhausen, B. Lorenz, H. Zhu, W. Geurtsen, R. Bohnensack, W.E.G. Müller, H.C. Schröder, J. Bone Miner. Res. 13 (1998) 803–812.
[23] W.E.G. Müller, M. Ackermann, B. Al-Nawas, L.A.R. Righesso, R. Muñoz-Espí, E. Tolba, M. Neufurth, H.C. Schröder, X.H. Wang, Acta Biomater. 118 (2020) 233–247.
[24] X.H. Wang, M. Ackermann, E. Tolba, M. Neufurth, F. Wurm, Q.L. Feng, S.F. Wang, H.C. Schröder, W.E.G. Müller, Eur. Cells Mater. 32 (2016) 271–283.
[25] W.E.G. Müller, M. Ackermann, S.F. Wang, M. Neufurth, R. Muñoz-Espí, Q.L. Feng, H.C. Schröder, X.H. Wang, Cell. Mol. Life Sci. 75 (2018) 21–32.
[26] W.E.G. Müller, D. Relkovic, M. Ackermann, S.F. Wang, M. Neufurth, A. Paravic-Radicevic, H. Ushijima, H.C. Schröder, X.H. Wang, Polymers 9 (2017) 300.
[27] H. Schepler, M. Neufurth, S.F. Wang, Z.D. She, H.C. Schröder, X.H. Wang, W.E.G. Müller, Theranostics 12 (2022) 18–34.
[28] B. Lorenz, H.C. Schröder, Biochim. Biophys. Acta 1547 (2001) 254–261.
[29] F. Lippman, Adv. Enzymol. 1 (1941) 99–162.
[30] W.E.G. Müller, E. Tolba, Q.L. Feng, H.C. Schröder, J.S. Markl, M. Kokkinopoulou, X.H. Wang, J. Cell Sci. 128 (2015) 2202–2207.
[31] W.E.G. Müller, S.F. Wang, M. Neufurth, M. Kokkinopoulou, Q.L. Feng, H.C. Schröder, X.H. Wang, J. Cell Sci. 130 (2017) 2747–2756.
[32] P. Wan, X.P. Liu, Y. Xiong, Y.P. Ren, J. Chen, N.H. Lu, Y. Guo, A.P. Bai, Sci. Rep. 6 (2016) 19108.
[33] H.E. Burrell, B. Wlodarski, B.J. Foster, K.A. Buckley, G.R. Sharpe, J.M. Quayle, A.W. Simpson, J.A. Gallagher, J. Biol. Chem. 280 (2005) 29667–29676.
[34] S.P. Apell, M. Neidrauer, E.S. Papazoglou, V. Pizziconi, Med. Phys. (2012) https://arxiv.org/abs/1212.3778.
[35] B. Dalisson, J. Barralet, Adv. Healthc. Mater. 8 (2019) e1900764.
[36] Y.Q. Mo, H. Sarojini, R. Wan, Q.W. Zhang, J.P. Wang, S. Eichenberger, G.J. Kotwal, S. Chien, Front. Pharmacol. 10 (2020) 1502.
[37] W.E.G. Müller, H.C. Schröder, X.H. Wang, Chem. Rev. 119 (2019) 12337–12374.
[38] P.A. Borges, I. Waclawiak, J.L. Georgii, V.D.S. Fraga-Junior, J.F. Barros, F.S. Lemos, T. Russo-Abrahão, E.M. Saraiva, C.M. Takiya, R. Coutinho-Silva, C. Penido, C. Mermelstein, J.R. Meyer-Fernandes, F.B. Canto, J.S. Neves, P.A. Melo, C. Canetti, C.F. Benjamim, Front. Immunol. 12 (2021) 651740.
[39] D.G. Smith, W.J. Mills, R.G. Steen, D. Williams, Foot Ankle Int. 20 (1999) 258–262.
[40] L.J. Bessa, P. Fazii, M. Di Giulio, L. Cellini, Int. Wound J. 12 (2015) 47–52.
[41] F. Bagnoli, R. Rappuoli, G. Grandi, *Staphylococcus aureus*: Microbiology, Pathology, Immunology, Therapy and Prophylaxis, Springer-Nature, Cham, Switzerland, 2017.
[42] P. Basso, M. Ragno, S. Elsen, E. Reboud, G. Golovkine, S. Bouillot, P. Huber, S. Lory, E. Faudry, I. Attrée, mBio 8 (2017) 16 e02250-.
[43] V. Tóth, L. Emódy, Acta Microbiol. Immunol. Hung. 47 (2000) 457–470.
[44] D. Roderer, S. Benke, B. Schuler, R. Glockshuber, J. Biol. Chem. 291 (2016) 5652–5663.
[45] G. Menestrina, M. Dalla Serra, M. Comai, M. Coraiola, G. Viero, S. Werner, D.A. Colin, H. Monteil, G. Prévost, FEBS Lett. 552 (2003) 54–60.
[46] I. Walev, E. Martin, D. Jonas, M. Mohamadzadeh, W. Müller-Klieser, L. Kunz, S. Bhakdi, Infect. Immun. 61 (1993) 4972–4979.
[47] M. Dal Peraro, F.G. van der Goot, Nat. Rev. Microbiol. 14 (2016) 77–92.
[48] Y. Eguchi, S. Shimizu, Y. Tsujimoto, Cancer Res. 57 (1997) 1835–1840.
[49] W.E.G. Müller, S.F. Wang, E. Tolba, M. Neufurth, M. Ackermann, R. Muñoz-Espí, I. Lieberwirth, G. Glasser, H.C. Schröder, X.H. Wang, Small 14 (2018) e1801170.
[50] W.E.G. Müller, E. Tolba, S.F. Wang, M. Neufurth, I. Lieberwirth, M. Ackermann, H.C. Schröder, X.H. Wang, Sci. Rep. 10 (2020) 17147.
[51] G.F. El Fawal, M.M. Abu-Serie, M.A. Hassan, M.S. Elnouby, Int. J. Biol. Macromol. 111 (2018) 649–659.
[52] S. Jain, M. Sengupta, S. Sarkar, S. Ghosh, A.N. Mitra, A. Sinha, S. Chakravorty, J. Clin. Diagn. Res. 10 (2016) DC22.
[53] S. Harrington, L. Ott, F. Karanu, K. Ramachandran, L. Stehno-Bittel, Tissue Eng. Part A 27 (2021) 153–164.
[54] H. Zhang, X.Y. Sun, J. Wang, Y.L. Zhang, M.N. Dong, T. Bu, L.H. Li, Y.N. Liu, L. Wang, Adv. Funct. Mater. 31 (2021) 2100093.
[55] L.H.P. Pham, L. Bautista, D.C. Vargas, X.L. Luo, RSC Adv. 8 (2018) 30441–30447.
[56] R.L. Panton, Incompressible Flow, 4th ed., Wiley Press, Hoboken, NJ, USA, 2013.
[57] J. Connolly, E. Boldock, L.R. Prince, S.A. Renshaw, M.K. Whyte, S.J. Foster, Infect. Immun. 85 (2017) 17 e00337-.
[58] D.M. Missiakas, O. Schneewind, Curr. Protoc. Microbiol. 28 (2013) 9C.1.1–9C.1.9.
[59] W.E.G. Müller, M. Ackermann, M. Neufurth, E. Tolba, S.F. Wang, Q.L. Feng, H.C. Schröder, X.H. Wang, Polymers 9 (2017) 120.
[60] W.E.G. Müller, R.K. Zahn, B. Kurelec, C. Lucu, I. Müller, G. Uhlenbruck, J. Bacteriol. 145 (1981) 548–558.
[61] W.E.G. Müller, M. Neufurth, E. Tolba, M. Ackermann, M. Korzhev, S.F. Wang, Q.L. Feng, H.C. Schröder, X.H. Wang, Dent. Mater. 33 (2017) 753–764.
[62] P. Vaudaux, E. Huggler, W. Rhys-Williams, W.G. Love, D.P. Lew, Int. J. Antimicrob. Agents 37 (2011) 576–579.
[63] J. Cao, M. Su, N. Hasan, J. Lee, D. Kwak, D.Y. Kim, K. Kim, E.H. Lee, J.H. Jung, J.W. Yoo, Pharmaceutics 12 (2020) 926.
[64] M. Herten, T. Bisdas, D. Knaack, K. Becker, N. Osada, G.B. Torsello, E.A. Idelevich, Front. Microbiol. 8 (2017) 2333.
[65] M. Damen, L. Wirtz, E. Soroka, H. Khatif, C. Kukat, B.D. Simons, H. Bazzi, Nat. Commun. 12 (2021) 3227.
[66] V. Karantza, Oncogene 30 (2011) 127–138.
[67] W.E.G. Müller, R.K. Zahn, Cancer Res. 39 (1979) 1102–1107.
[68] S.F. Wang, X.H. Wang, M. Neufurth, E. Tolba, H. Schepler, S.C. Xiao, H.C. Schröder, W.E.G. Müller, Molecules 25 (2020) 5210.
[69] W.E.G. Müller, M. Neufurth, S.F. Wang, H.C. Schröder, X.H. Wang, Cancers 13 (2021) 750.
[70] W.E.G. Müller, S.F. Wang, M. Ackermann, T. Gerich, M. Wiens, M. Neufurth, H.C. Schröder, X.H. Wang, Adv. Funct. Mater. 29 (2019) 1905220.
[71] C.L. Chen, W.H. Hou, I.H. Liu, G. Hsiao, S.S. Huang, J.S. Huang, J. Cell Sci. 122 (2009) 1863–1871.
[72] T. Friis, A.M. Engel, C.D. Bendiksen, L.S. Larsen, G. Houen, Cancers 5 (2013) 762–785 (Basel).
[73] N. Kurebayashi, T. Kodama, Y. Ogawa, J. Biochem. 88 (1980) 871–876.
[74] V. Rangaraju, N. Calloway, T.A. Ryan, Cell 156 (2014) 825–835.
[75] W. Strober, Curr. Protoc. Immunol. (2001) Appendix 3, Appendix 3B, doi:10.1002/0471142735.ima03bs21.
[76] S. Gaucher, M. Jarraya, Cell Tissue Bank. 16 (2015) 325–329.
[77] M. Sonnaert, I. Papantoniou, F.P. Luyten, J.I. Schrooten, Tissue Eng. Part C Methods 21 (2015) 519–529.
[78] WMA declaration of Helsinki – Ethical principles for medical research involving human subjects, World Medical Association, Ferney-Voltaire, France, June 2022 https://www.wma.net/policies-post/wma-declaration-of-helsinki-ethical-principles-for-medical-research-involving-human-subjects/.
[79] L.M. Lugo, P. Lei, S.T. Andreadis, Tissue Eng. Part A 17 (2011) 665–675.
[80] K.D. Sumigray, T. Lechler, Mol. Biol. Cell 23 (2012) 792–799.
[81] K. Lange, J. Cell. Physiol. 226 (2011) 896–927.
[82] P. Martin, R. Nunan, Br. J. Dermatol. 173 (2015) 370–378.
[83] L. Paragh, D. Törőcsik, Biomed. Res. Int. 2017 (2017) 3571861.
[84] J.A. Thackham, D.L. McElwain, R.J. Long, Wound Repair Regen. 16 (2008) 321–330.
[85] L.M. Schiffmann, J.P. Werthenbach, F. Heintges-Kleinhofer, J.M. Seeger, M. Fritsch, S.D. Günther, S. Willenborg, S. Brodesser, C. Lucas, C. Jüngst, M.C. Albert, F. Schorn, A. Witt, C.T. Moraes, C.J. Bruns, M. Pasparakis, M. Krönke, S.A. Eming, O. Coutelle, H. Kashkar, Nat. Commun. 11 (2020) 3653.
[86] Y. Guan, H. Niu, Z.T. Liu, Y. Dang, J. Shen, M. Zayed, L. Ma, J.J. Guan, Sci. Adv. 7 (2021) eabj0153.
[87] Z.Y. Yang, H.H. Chen, P.Z. Yang, X.F. Shen, Y.Q. Hu, Y.H. Cheng, H.W. Yao, Z.T. Zhang, Biomaterials 282 (2022) 121401.
[88] J. Song, N. Pfanner, T. Becker, Proc. Natl. Acad. Sci. U. S. A. 115 (2018) 2850–2852.
[89] J.H. Morrissey, S.H. Choi, S.A. Smith, Blood 119 (2012) 5972–5979.
[90] F. Eisinger, J. Patzelt, H.F. Langer, Front. Med. 5 (2018) 317 (Lausanne).
[91] B. Nocek, S. Kochinyan, M. Proudfoot, G. Brown, E. Evdokimova, J. Osipiuk, A.M. Edwards, A. Savchenko, A. Joachimiak, A.F. Yakunin, Proc. Natl. Acad. Sci. U. S. A. 105 (2008) 17730–17735.
[92] W.E.G. Müller, H. Schepler, E. Tolba, S.F. Wang, M. Ackermann, R. Muñoz-Espí, S.C. Xiao, R.W. Tan, Z.D. She, M. Neufurth, H.C. Schröder, X.H. Wang, J. Mater. Chem. B 8 (2020) 5892–5902.
[93] H. Sarojini, A. Bajorek, R. Wan, J. Wang, Q. Zhang, A.T. Billeter, S. Chien, Front. Pharmacol. 12 (2021) 594586.
[94] G. Burnstock, Brain Neurosci. Adv. 2 (2018) 1–10.

[95] O.I. Parisi, F. Puoci, D. Restuccia, G. Farina, F. Lemma, N. Picci, Polyphen. Hum. Health Dis. 1 (2014) 29–45.
[96] K.J. Thomas, C.V. Rice, Biometals 27 (2014) 1361–1370.
[97] L.A. Mamedov, A.V. Nikolaev, V.V. Zakharov, A.B. Shekhter, Y.R. Khrust, Bull. Exp. Biol. Med. 104 (1987) 1233–1236.
[98] A. Kitamura, T. Minematsu, G. Nakagami, H. Sanada, SAGE Open Med. 6 (2018) 1–9.
[99] X. Zhang, C.H. Ren, F. Hu, Y. Gao, Z.Y. Wang, H.Q. Li, J.F. Liu, B. Liu, C.H. Yang, Anal. Chem. 92 (2020) 5185–5190.
[100] E.N. Maldonado, J.J. Lemasters, Mitochondrion A 19 (2014) 78–84.
[101] T.B. McEwan, R.A. Sophocleous, P. Cuthbertson, K.J. Mansfield, M.L. Sanderson--Smith, R. Sluyter, Life Sci. 283 (2021) 119850.
[102] R. Baaske, M. Richter, N. Möller, S. Ziesemer, I. Eiffler, C. Müller, J.P. Hildebrandt, Toxins 8 (2016) 365 (Basel).
[103] Y.F. Cui, Y.Y. Wang, M. Liu, L. Qiu, P. Xing, X. Wang, G.G. Ying, B.H. Li, J. Mol. Cell. Biol. 9 (2017) 395–408.
[104] R. Yamanaka, S. Tabata, Y. Shindo, K. Hotta, K. Suzuki, T. Soga, K. Oka, Sci. Rep. 6 (2016) 30027.
[105] R. Stefureac, Y.T. Long, H.B. Kraatz, P. Howard, J.S. Lee, Biochemistry 45 (2006) 9172–9179.
[106] M. Neufurth, X.H. Wang, H.C. Schröder, Q.L. Feng, B. Diehl-Seifert, T. Ziebart, R. Steffen, S.F. Wang, W.E.G. Müller, Biomaterials 35 (2014) 8810–8819.
[107] C.M. Simbulan-Rosenthal, A. Gaur, V.A. Sanabria, L.J. Dussan, R. Saxena, J. Schmidt, T. Kitani, Y.S. Chen, S. Rahim, A. Uren, E. Crooke, D.S. Rosenthal, Exp. Dermatol. 24 (2015) 636–639.
[108] X.H. Wang, H.C. Schröder, W.E.G. Müller, J. Mat. Chem. B 6 (2018) 2385–2412.
[109] S. Bru, J.M. Martínez-Laínez, S. Hernández-Ortega, E. Quandt, J. Torres-Torronteras, R. Martí, D. Canadell, J. Ariño, S. Sharma, J. Jiménez, J. Clotet, Mol. Microbiol. 101 (2016) 367–380.
[110] H. Ando, Y. Niki, M. Ito, K. Akiyama, M.S. Matsui, D.B. Yarosh, M. Ichihashi, J. Invest. Dermatol. 132 (2012) 1222–1229.
[111] C. Lindholm, R. Searle, Int. Wound J. Suppl. 13 (2016) 5–15.
[112] E. Darwin, M. Tomic-Canic, Curr. Dermatol. Rep. 7 (2018) 296–302.
[113] S. Barrientos, O. Stojadinovic, M.S. Golinko, H. Brem, M. Tomic-Canic, Wound Repair Regen. 16 (2008) 585–601.
[114] H. Kawamura, T. Kawamura, Y. Kanda, T. Kobayashi, T. Abo, Immunology 136 (2012) 448–458.
[115] A. Ben-Baruch, D.F. Michiel, J.J. Oppenheim, J. Biol. Chem. 270 (1995) 11703–11706.